active not only in germ cells, but also in somatic cells if innate protection system would not work appropriately. The mechanism by which L1 transpositions are restricted in the normal cells, however, remains unknown.

Here we examined whether antiretroviral innate proteins, human A3 (hA3) family members are able to show inhibitory effects on L1 retrotransposon. hA3 family, in particular, hA3A, hA3B, hA3F and hA3G protein expressions strongly decrease the transposition level of L1 elements that does not correlate with either antiretroviral activity or patterns of subcellular localization. Results of DNA sequencing argue that inhibitory effect of hA3 family on L1 transposition might be independent of deaminase activity. We conclude that all hA3 proteins are able to differentially suppress uncontrolled transposition of L1 retroelements.

MATERIALS AND METHODS

DNA constructs

The Vif-deficient HIV-1 proviral indicator construct pNL-Luc-F(-)E(-), and the L1 indicator constructs $pL1_{RP}$-EGFP (kindly provided by E.T. Luning Prak) and pCEP4/L1mneoI/ColE1 (kindly provided by N. Gilbert) have previously been described elsewhere (37–39). Total RNA was isolated from H9 cells by using RNAqueous Kit (Ambion), and was subjected to reverse transcription, followed by amplification with oligonucleotides 5′-GGG GTA CCA TGA ATC CAC AGA TCA GAA ATC CG-3′/5′-ATT CTC GAG CTG GAG AAT CTC CCG TAG CCT TC-3′, 5′-GGG GTA CCA TGA AGC CTC ACT TCA GAA AC-3′/5′-CCG CTC GAG AAT CTC CTG CAG CTT GC-3′, 5′-GGG GTA CCA TGA AGC CTC ACT TCA GAA ACA-3′/5′-CCG CTC GAG GTT TTC CTG ATT CTG GAG AAT-3′ and 5′-GGG GTA CCA TGG CTC TGT TAA CAG CCG AAA CAT TCC G-3′/5′-CCG CTC GAG GGA CTG CTT TAT CCT CTC AAG-3′, producing hA3DE, hA3F, hA3G or hA3H fragments, respectively. Total RNA isolated from HeLa cells was subjected to RT-PCR amplification of hA3A, hA3B or hA3C genes using oligonucleotides 5′-ATG GTA CCA TGG AAG CCA GCC CAG CAT C-3′/5′-CAT CTC GAG GTT TCC CTG ATT CTG GAG AAT GG-3′, 5′-GGG GTA CCA TGA ATC CAC AGA TCA GAA ATC CG-3′/5′-CCG CTC GAG GTT TCC CTG ATT CTG GAG AAT GG-3′, 5′-GGG GTA CCA TGA ATC CAC AGA TCA GAA AC-3′/5′-ATT CTC GAG CTG GAG ACT CTC CCG TAG CCT TC-3′, respectively. Amplified hA3 fragments were KpnI/XhoI-digested and cloned into a modified mammalian expression plasmid pCAGGS carrying carboxy-terminal hemaggulutinin (HA)-tag. To generate an indicator retrovector construct pMSCVneo-Luc, a luciferase gene from pGL4.10[luc2] vector (Promega) was PCR-amplified by using oligonucleotides 5′-GGA ATT CGC CAT GGA AGA TGC CAA AAA CAT-3′/5′-AAT CTC GAG TTA CAC GGC GAT CTT GCC GCC C-3′, digested with EcoRI and XhoI restriction enzymes, and inserted into pMSCVneo (Clontech). All constructs were verified by DNA sequencing.

Cell maintenance, transfections and protein analyses

HeLa cells, 293T cells and HT1080 cells were maintained as described elsewhere (40,41). The human osteocarcinoma 143BTK- cells were kindly provided by J. Hayashi and cultured as previously described (42). 293T cells were transfected with HA-tagged hA3 plasmids by using FuGENE 6 transfection reagent (Roche) to confirm hA3 protein expressions. Cell extracts from transfected cells are subjected to western analysis using an anti-HA mouse monoclonal antibody (Sigma). HeLa cells were transfected with the same constructs by using Lipofectamine with Plus reagents (Invitrogen) to determine subcellular localization of hA3 proteins. Cells were fixed, permeabilized and incubated with an anti-HA monoclonal antibody and Alexa 488 conjugating anti-mouse IgG (Invitrogen) used for the first and second antibodies, respectively. Microscopic observation was performed by using FV-1000 confocal microscopy (Olympus).

Viral infectivity assay

To prepare MuLV or HIV-1 supernatants, 7×10^5 293T cells were cotransfected with 0.1 μg of hA3 expression plasmids and 0.1 μg of VSV-G expression plasmid pHIT/G (43), together with either 0.9 μg of pMSCVneo-Luc and 0.9 μg of retroviral packaging vector pVPack-GP (Stratagene), or 1 μg of pNL-Luc-F(-)E(-) by using FuGENE 6 and 0.8 μg of an empty vector. Sixteen hours later, cells were washed with phosphate-buffered saline, and then 2 ml of fresh complete medium was added. After 24 h, supernatants were harvested and treated with 37.5 U/ml DNase I (Roche) for 37°C for 30 min. HIV-1 supernatants were subjected to measure p24 antigen by HIV-1 p24-antigen capture enzyme linked immunosorbent assay (RETRO-TEK). To normalize MuLV supernatants, transfected cells were lysed in 100 μl of passive lysis buffer (Promega), and firefly luciferase activities which indicate transfection efficiencies were determined by Centro LB960 (Berthold). To determine the infectivity, 1×10^4 293T cells were incubated with 0.1 ng of p24 antigen of each HIV-1 or 100 μl of normalized MuLV supernatants. After 48 h, cells were lysed in 100 μl of lysis buffer, and firefly luciferase activities were determined as described above.

L1 retrotransposition assay

L1 retrotransposition assay was performed by cotransfection of 3.5×10^5 293T cells with 0.1 μg of the respective hA3 expression plasmids, 0.5 μg of EGFP-based L1 reporter vector $pL1_{RP}$-EGFP and 0.4 μg of an empty vector. Transfected cells were maintained by puromycin treatment (0.5 μg/ml) for 10 days. EGFP expression resulting from retrotransposition was verified by flow cytometry. Another L1 retrotransposition assay was performed by cotransfection of HeLa cells with equal amounts of the respective hA3 expression plasmids and neomycin-resistant (*neo*′)-based L1 reporter vector pCEP4/L1mneoI/ColE1, as previously described (15). After 72 h, cells were trypsinized, re-seeded onto 100 mm dishes for G418 (1 mg/ml) selection and maintained. Fourteen days after selection, resultant G418-resistant

($G418^R$) colonies were fixed, stained with crystal violet (Merck), and counted.

Confirmation of *de novo* L1 copy number

Presumed copy number of retrotransposed L1 elements was determined by real-time PCR targeting the EGFP gene. Ten days after transfection as described above, total cellular DNA was extracted from 293T cells by using DNeasy kit (Qiagen) which is able to recover both chromosomal and episomal DNA (according to the manufacture's manual). One hundred nanograms of each DNA was subjected to real-time PCR detection using oligonucleotides 5′-GAA GAA CGG CAT CAA GGT GAA C-3′/5′-GGT GCT CAG GTA GTG GTT GTC-3′ and a probe 6-carboxyfluorescein (FAM)-5′-AGC GTG CAG CTC GCC GAC CA-3′- black-hole quencher 1 (BHQ1). Real-time PCR was performed by using ABI 7900HT (ABI). L1 DNA levels are presented as copies per 10^4 cells.

Determination of endogenous levels of L1 and hA3 mRNA expressions in cell lines

Real-time RT-PCR was performed to quantify the endogenous level of L1 and hA3 mRNA expression (and of glyceraldehyde-3-phosphate-dehydrogenase [GAPDH] mRNA expression as an internal control) in various cell types. Total RNA was extracted from peripheral blood lymphocytes (PBL; from two different donors), 293T, HeLa, HT1080 and 143BTK- cells, by using RNAqueous Kit, and then, treated with TURBO DNA-*free* (Ambion) according to the manufacturer's protocols. Specific oligonucleotides (o) and probes (p) used are as follows: L1, (o) 5′-GAG AAC AAA GAC ACC ACA TAC C-3′/5′-GGC ATT TAG TGC TAT AAA TTT CCC -3′ (p) FAM-5′-TCT CTG GGA CGC ATT CAA AGC AGT-3′-BHQ1; hA3A, (o) 5′-CAC ACA TAT TCA CTT CCA ACT TTA AC-3′/5′-GTC CAG GCG CTC CAC TTC-3′ (p) FAM-5′-CAT TGG AAG GCA TAA GAC CTA CCT GTG C-3′-BHQ1; hA3B, (o) 5′-CGC TAA AGG AGA TTC TCA GAT ACC-3′/5′-CAG GAC CCA GGT GCC ATT G-3′ (p) FAM-5′-CCA GGC GCT CCA CCT CAT AGC ACA-3′-BHQ1; hA3C, (o) 5′-CTG TGC TTC ACC GTG GAA GG-3′/5′-TGA CAA TGG GTC TCA GAA TCC AC-3′ (p) FAM-5′-AGC GCC GCT CAG TTG TCT CCT GGA-3′-BHQ1; hA3DE, (o) 5′-ACC GCA CGC TAA AGG AGA TTC-3′/5′-CGA CCA CAG GCT TTC AGT AGG-3′ (p) FAM-5′-ACC CGA TGG AGG CAA TGT ACC CAC AC-3′-BHQ1; hA3F, (o) 5′-TGC CTT GGT ACA AAT TCG ATG AC-3′/5′-AGT GGA AGT AGA ATA TGT GTG GAT AC-3′ (p) FAM-5′-ATT CCT GCA CCG CAC GCT AAA GGA GA-3′-BHQ1; hA3G, (o) 5′-GGC CGA GGA CCC GAA GG-3′/5′-TTC TGA CAC AGG CTG CGA AG-3′ (p) FAM-5′-CCC TGA CCA TCT TCG TTG CCC GCC-3′-BHQ1; hA3H, (o) 5′-GGC TCA CGA CCA TCT GAA CC-3′/5′-AGT CAG CAA ACT CTG GGA AGC-3′ (p) FAM-5′-CGC CTC CCG CCT GTA CTA CCA CTG G-3′-BHQ1; GAPDH (o) 5′-GAT GCT GGC GCT GAG TAC G-3′/5′-GCA GAG ATG ATG ACC CTT TTG G-3′ (p) FAM-5′-TGG AGT CCA CTG GCG TCT TCA CCA CC-3′-BHQ1. Oligonucleotide specificity for each hA3 sequence was confirmed by simultaneously using all hA3 plasmids which gave no non-specific signals. L1 and hA3 mRNA levels were normalized with GAPDH mRNA levels.

Sequencing of *de novo* L1 genes

Total cellular DNAs were isolated by using DNeasy from the cells at 2 and 6 days after cotransfection of $pL1_{RP}$-EGFP with either an empty vector or hA3 constructs. Intronless EGFP DNAs were nested-PCR-amplified by using PfxUltima (Invitrogen) and cloned into pCR-Blunt vector using Zero Blunt® PCR Cloning Kit (Invitrogen). Sequencing was performed by using ABI3130 (ABI).

RESULTS AND DISCUSSION

We first examined if L1 is endogenously expressed in primary and established cells. To do this, we performed real-time RT-PCR targeting ORF1 gene, using total RNA derived from two primary lymphocytes from different donors and from four different established cell lines. As shown in Figure 1, although the expression levels vary among the cells tested, we found that all the cells express L1 mRNA at the level of 10–100 copies/cell. The results strongly emphasize that, even though L1 is expressed in normal cells, its reverse transcription and integration should be blocked by some innate protection system. We therefore hypothesized that antiretroviral innate proteins, hA3 family, might be effective on L1 retrotransposition as well as on that of mouse retroelements (15).

To test this hypothesis, we created HA-tagged hA3 expression plasmids, using cDNA reverse-transcribed from total RNA of H9 cells, or HeLa cells. Protein expressions in the cells transfected with each plasmid were confirmed by immunoblotting using anti-HA antibodies (Figure 2A). Using these plasmids, subcellular localization

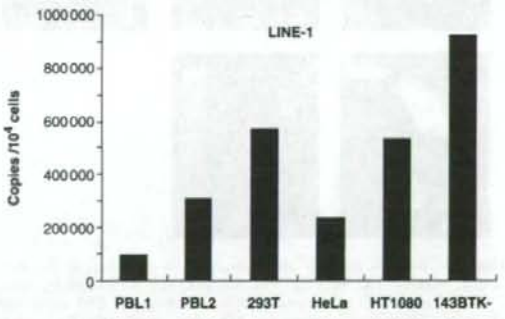

Figure 1. Endogenous expression of LINE-1 in primary and established cells. LINE-1 mRNA copy numbers in PBL (two different donors), 293T, HeLa, HT1080 and 143BTK- cells were determined by real-time RT-PCR using total RNAs isolated from those cells. L1 mRNA levels were normalized with GAPDH mRNA levels, and are presented as copies per 10^4 cells.

of hA3 proteins was determined by immunofluorescence microscopy. As shown in Figure 2B, results were consistent with the molecular size of each protein, i.e. ~46 kDa proteins, which are larger than nuclear pore exclusion limit (44), hA3DE, hA3F and hA3G proteins, localized into the cytoplasm, while ~23 kDa proteins, which are smaller than the limit, hA3A, hA3C and hA3H, passively diffused into the nucleus. Although a larger protein, hA3B was exceptionally found in the nucleus, this localization is consistent with the recent report that hA3B harbors a nuclear localization signal (45).

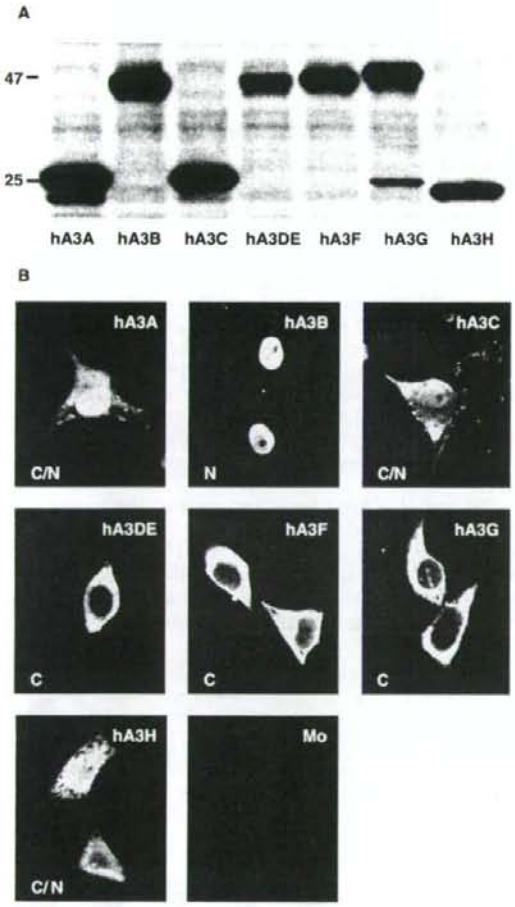

Figure 2. Western analysis and subcellular localization of the hA3 family proteins. (**A**) Western blot analysis was performed by using extracts from 293T cells transfected with HA-tagged hA3 expression plasmids. Antibodies specific for HA were used. (**B**) To analyze subcellular localization of hA3 proteins, immunofluorescence microscopy was performed by using HeLa cells transfected with the HA-tagged hA3 expression plasmids. An anti-HA monoclonal antibody and Alexa 488 conjugating anti-mouse IgG were used for the first antibody and for the second antibody, respectively. C, N or C/N in the pictures indicates cytoplasmic, nuclear or both localizations, respectively.

We next examined inhibitory effects of hA3 family proteins on Vif-deficient HIV-1 and MuLV. Using virions from the cells cotransfected with each virus construct and hA3 expression plasmids, we determined infectivity reduction by hA3 proteins. In accordance with the previous reports (2,3,39,46–51), hA3B and hA3F as well as hA3G revealed robust inhibitory activity on HIV-1, while hA3C and hA3DE showed partial activity (Figure 3A). MuLV infectivity was reduced by hA3B, hA3C and hA3G protein expressions (Figure 3B), as previously reported (2,49,50). Therefore, with respect to the antiretroviral activity, we here confirmed known phenotypes of all hA3 family members as observed in these experiments.

To determine if hA3 family members are able to inhibit L1 retrotransposition, we first employed EGFP-based retrotransposition assay (38). In this assay system, we utilized a L1 clone DNA carrying a reverse-oriented EGFP gene separated by a gamma-globin intron, and also carrying a puromycin resistance gene which allows selection of transfected cells. After transfection of the cells with this construct, followed by puromycin selection, EGFP with L1 is transcribed, spliced, reverse-transcribed and integrated. Then, the EGFP integrated with L1 is driven by CMV promoter and expressed. In other words, EGFP-positive cells are the cells in which L1

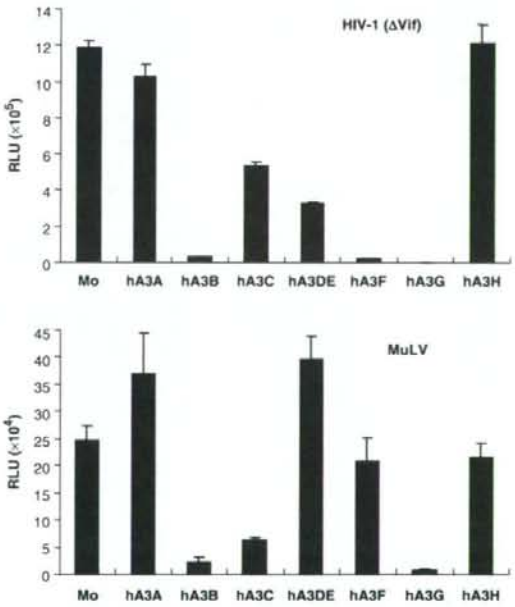

Figure 3. Inhibitory effect of hA3 family proteins on retroviruses. 293T cells were cotransfected with VSV-G and hA3 expression plasmids, together with a luciferase-based HIV-1 or MuLV construct. After 48 h, each viral supernatant was harvested. Normalized supernatants were incubated with 293T cells for additional 48 h. Cells were then lysed and subjected to luciferase assay. Data shown are mean ± SD. RLU: relative light units.

retrotransposition successfully occurred. EGFP expression in cells cotransfected with each hA3 plasmid and the L1-EGFP vector were visualized by microscopy (Figure 4A), and quantitatively analyzed by flow cytometry (Figure 4B). Without coexpressions of hA3 proteins, L1 transposition normally occurred at the level shown in the upper left panel of Figure 4. In contrast, coexpressions of any of hA3 proteins differentially inhibited L1 retrotransposition, and in particular, hA3A, hA3B, hA3F and hA3G expressions strongly decreased the transposition level of L1 elements to 0.9, 14.0, 15.6 and 10.2%, respectively. These activities against L1 did not correlate with their patterns of subcellular localization (Figure 2B) and inhibitory activities on retroviruses (Figure 3A and B). In this assay, we observed no cytotoxic effect of A3 proteins (data not shown) as previously reported (52,53).

To assess reproducibility of this experiment, we next performed a different type of retrotransposition assay, using L1 vector which carries *neo*^{r} gene (37) instead of the EGFP gene. In this assay, after neomycin selection following transfection, we were able to quantify the retrotransposition level, simply by counting G418^r colonies. As shown in Figure 5A and B, this assay gave results equivalent to that obtained with EGFP-based assay. Thus, on the basis of the data presented here, we conclude that all hA3 proteins act to differentially suppress uncontrolled L1 retrotransposition. Importantly, in striking contrast to the recent reports (45,53–56), we observed the inhibitory effect of hA3G proteins on retrotransposition in both assays (Figures 4 and 5).

To confirm that hA3G is indeed effective on retrotransposition inhibition, we next measured presumed copy number of retrotransposed L1 elements by performing real-time PCR using total DNA which was isolated from the cells used in Figure 4. To exclude detection of genomic DNA, we targeted intronless EGFP DNA which is detectable only in spliced and reverse-transcribed L1 elements carrying the EGFP gene. As shown in Figure 6, results obtained with this assay were fully consistent with those observed in flow cytometry analysis, and in neo-resistance assay. We therefore conclude that hA3G is indeed able to inhibit L1 retrotransposition as well as hA3A, hA3B and hA3F. Importantly, the fact that results shown in Figure 6 were obtained by detecting not only integrants, but also reverse transcripts, and are

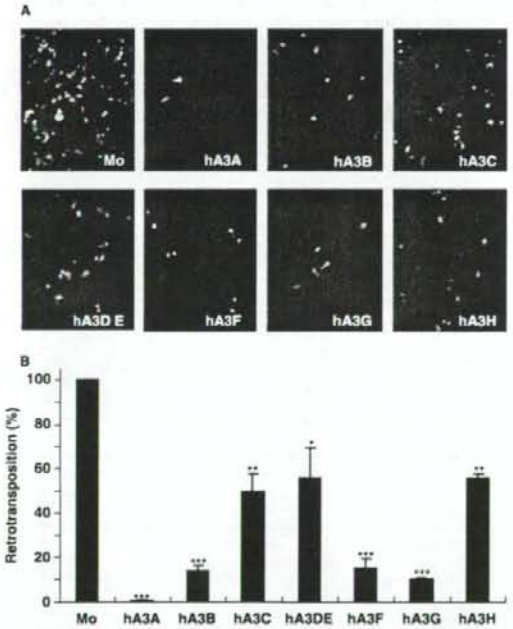

Figure 4. EGFP-based retrotransposition assay. 293T cells were cotransfected with the EGFP-based L1 retrotransposon indicator construct pL1$_{RP}$-EGFP and hA3 expression plasmids. After 48 h, cells were subjected to puromycin (0.5 μg/ml) selection. After 8 days of puromycin selection, cells were observed by fluorescence microscopy (**A**) and subjected to flow cytometry analysis (**B**). Retrotransposition level in the absence of hA3 proteins was set as 100%. Data shown are mean ± SD; $^*P<0.05$, $^{**}P<0.01$, $^{***}P<0.001$, *t*-test.

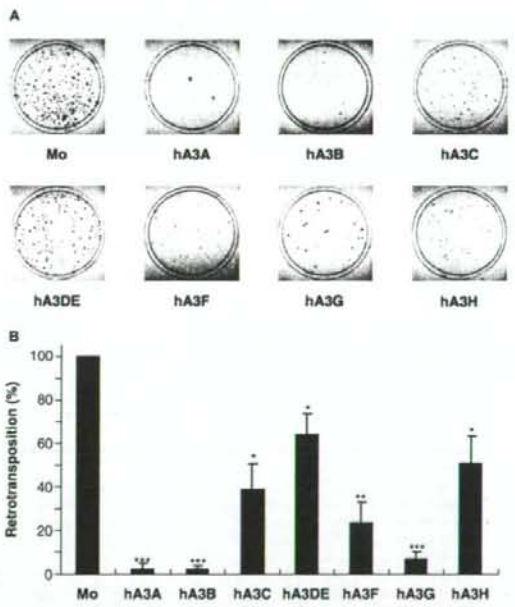

Figure 5. *neo*^{r}-based retrotransposition assay. HeLa cells were cotransfected with pCEP4/L1mneoI/ColE1 and the respective hA3 expression plasmids. Seventy-two hours later, cells were trypsinized, re-seeded onto 100 mm dishes, and subjected to G418 (1 mg/ml) selection. Fourteen days after selection, resultant G418^R colonies fixed, stained with crystal violet (**A**), and counted to determine the level of L1 retrotransposition (**B**). Transposition level in the absence of hA3 proteins was set as 100%. Data shown are mean ± SD; $^*P<0.05$, $^{**}P<0.01$, $^{***}P<0.001$, *t*-test.

similar to those observed in Figure 4 in which levels of EGFP expression represent L1 integrants, suggest that hA3 proteins at least hA3A and hA3G suppress *de novo* L1 DNA synthesis, but not integration.

To examine whether cytidine deamination would explain the mechanism by which the retrotransposition is inhibited, we sequenced L1 elements resulting from retrotransposition which was reduced by hA3G protein. We targeted intronless reverse-oriented EGFP genes for the reason given above. Surprisingly, we observed only one C-to-T mutation (G-to-A mutation on plus-strand DNA) out of 4200 bp nucleotide sequences (Figure 7). As a control experiment, we analyzed deaminase activity of hA3G on Δvif HIV-1 reverse transcripts by sequencing the 3′ end of *env* genes in infected cells. In contrast to Figure 7, G-to-A mutations were found in 367 out of 5900 bp in total (unpublished data). In other hA3 protein expressions, we were not able to find any mutation (0 out of 25 200 bp, data not shown). These results suggest the possibility that inhibitory effect of hA3G on L1 retrotransposition might be independent of its deaminase activity as previously observed in studies of antiviral phenotypes (11,13,57), but this needs to be elucidated with further experiments using mutant hA3G, such as catalytically inactive mutants.

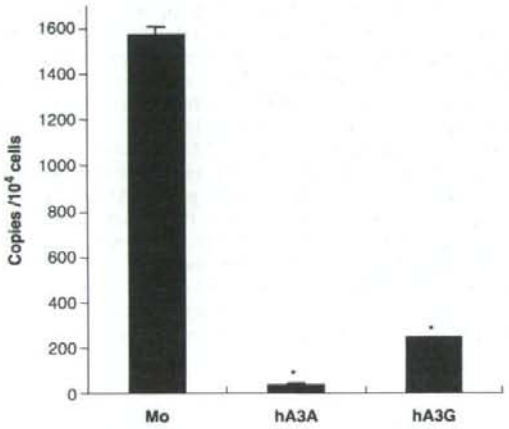

Figure 6. Real-time PCR targeting spliced EGFP genes. Total cellular DNA was extracted from the cells used in Figure 4 and subjected to real-time PCR analysis. Dual labeled probe was designed for the detection of spliced EGFP. Mock, hA3A and hA3G were shown as representatives. Data shown are mean ± SD; $^{*}P < 0.001$, *t*-test.

Finally, we performed real-time RT-PCR analysis to determine endogenous expression levels of hA3 proteins in various types of cells. As shown in Figure 8, we found that the endogenous levels of hA3 expressions vary depending on the cell types. Especially, some cell types abundantly coexpress hA3B and hA3G proteins which are able to effectively suppress L1 transposition. Therefore, the different results in other studies might be due to the different cells used.

In this study, we first presented evidence showing that primary and established cells endogenously express L1 mRNA at the level of 10–100 copies/cell. Although

Figure 7. Sequence analysis of L1 reverse transcripts. Total DNA was extracted from 293T cells cotransfected with $pL1_{RP}$-EGFP and hA3 expression plasmid, at 2 and 6 days after transfection. Reverse transcribed EGFP genes were PCR-amplified and inserted into the cloning vector. Alignment of partial sequences of EGFP genes in hA3G-cotransfected cells is shown.

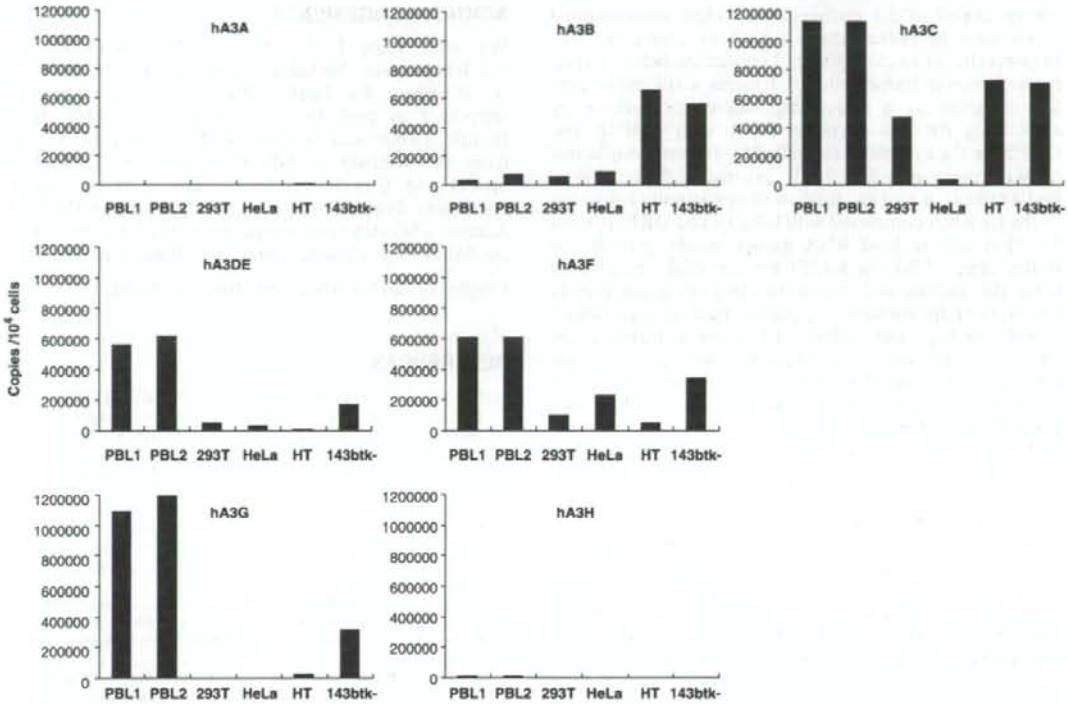

Figure 8. Endogenous expressions of hA3 family members in primary and established cells. Total RNAs were extracted from PBL (from two different donors), 293T, HeLa, HT1080 (HT) and 143BTK- cells, and subjected to real-time RT-PCR to determine the copy numbers of the respective hA3 mRNAs. Levels of hA3 mRNA were normalized with GAPDH mRNA levels, and are presented as copies per 10^4 cells.

we were unable to directly demonstrate endogenous expressions of L1 proteins *per se*, many, if not most, of L1 retroelements must be encoded from mRNA detected in our experiments, and should be sensitive to some innate immunity defenses. Otherwise, uncontrolled L1 transposition becomes obviously deleterious to the cells. Based on the hypothesis that hA3 family proteins of human innate antiretroviral factors might be the key to understanding how transposition of L1 retroelements is naturally inhibited in the cells, we preformed two different types of established retrotransposition assays using all hA3 (A, B, C, DE, F, G and H) expression plasmids. Results obtained in these assays revealed differential inhibitory effect of all hA3 family member proteins on L1 retrotransposition. However, we could not observe any correlation between the levels of L1 transposition inhibition by hA3 and either their subcellular localization or antiviral activities against retroviruses.

An intriguing finding in this study was that hA3G was also identified as an intrinsic inhibitor of L1 retrotransposition. This finding was indeed reproducible in two different retrotransposition assays, and a real-time PCR analysis. Sequence analysis, however, revealed no DNA deamination effect of hA3G on *de novo* L1 retrotransposons, strongly suggesting that cytidine deaminase hA3G inhibits L1 transposition by novel mechanism(s). Although we cannot rule out that hA3G might deaminate L1 reverse transcripts which could result in rapid degradation by cellular enzymes such as uracil DNA glycosylase and would be therefore undetectable, hA3G protein has been indeed found to have dual inhibitory effects on murine endogenous retroviruses, which are G-to-A editing and reduction of viral cDNA yields (58). Besides, antiretroviral function of hA3G has been demonstrated to be dissociated from its deaminase activity because deaminase mutants of hA3G still retained antiviral activity (59–61). Taken together, it is likely that hA3G could prevent L1 DNA synthesis *per se*. This still needs to be elucidated.

Cytoplasmic expression of hA3G protein, as observed in Figure 2B, has been thought to cause inaccessibility of this protein to L1 reverse transcripts which are synthesized in the nucleus, leading to the lack of inhibitory activity of hA3G on L1 transposition (45,56). Yet, another cytoplasmic hA3 family protein hA3F is reported to be also active on inhibition of L1 transposition (53,54), consistent with that observed in our study. This discrepancy might be explained by the mechanism of L1 replication as follows: L1 DNA synthesis in the nucleus is based on 'target-primed reverse transcription' in which reverse transcripts

are generated at L1 endonuclease-nicked chromosomal DNA using polyadenylated L1 RNA as a template (62). Importantly, at an early phase of replication before target-primed reverse transcription, L1 forms a ribonucleoprotein complex as a retrotransposition intermediate by associating its own encoding RNA with ORF1p and ORF2p in the cytoplasm (63–66). At this step, cytoplasmic hA3G protein as well as hA3F protein might be able to find a critical, if narrow, window of opportunity for access to the L1 RNA complexed with ORF1p and ORF2p, since hA3G is able to bind RNA nonspecifically (67). If this is the case, hA3G (or hA3F) protein might be able to enter the nucleus with the ribonucleoprotein complex in which ORF2p harbors a putative nuclear localization signal (68,69), and inhibit L1 reverse transcription effectively, by physically blocking the access of the ORF2p to the nicked chromosomal DNA, or by hindering the movement of the reverse transcriptase of ORF2p on a template L1 RNA.

Turelli *et al.* (56) originally reported that hA3G does not affect L1 retrotransposition in the EGFP-based retrotransposition assay which we also utilized in this article. The cells used in their experiments, 143BTK- osteocarcinoma cells, were found in our study to endogenously coexpress high level of hA3B and hA3G (Figure 8) which are able to effectively inhibit LINE-1 transposition. It seems likely that coexpression of hA3B and hA3G proteins might reduce the basal level of L1 retrotransposition. In fact, 143BTK- cells transfected with the $pL1_{RP}$-EGFP construct in our study showed only faint EGFP signals (data not shown) compared with those in 293T cells, although transfection efficiencies were equivalent in both the cells. Besides, reflecting phenotypes of cells expressing hA3B and hA3G proteins, 143BTK- cells transfected with an HIV-1 proviral construct with or without an intact *vif* gene produced ~50-fold less infectious virions, than did 293T cells (unpublished data). These virions showed no effect of Vif protein on infectivity rescue, just as described by Turelli *et al.* (56). This could be due to that hA3B which can be incorporated into virions as well as hA3G (48) might be more effective on inhibition of infection than does hA3G, leading to the lack of Vif-negative phenotypes.

The cell-type preference of hA3 protein expressions, however, might not be able to account for the results in three other articles very recently published, showing inability of hA3G to inhibit L1 transposition by using *neo*^{r}-based L1 retrotransposition assay in HeLa cells (45,53,55), as used in our study. A possible explanation can be drawn from the fact that HeLa cells are highly divergent (70) in which expression pattern of hA3 proteins might differ depending on derivatives of this cell line. Overall, this preferential hA3 expression in a cell type-dependent manner as observed in this study [and also in a tissue-specific manner described in other reports (1,17,46,48,49,51,71)] might explain the difference of results obtained. It will be of interest to further examine whether coexpression of hA3 proteins are able to either additively or cooperatively inhibit L1 retrotransposition.

ACKNOWLEDGEMENTS

We thank Eline T. Luning Prak, Nicolas Gilbert and Jun-Ichi Hayashi, for the kind gifts of reagents, and Mark A. Wainberg for helpful discussion. This work was supported in part by a grant from the Ministry of Health, Labor and Welfare of Japan and by a grant from the Ministry of Education, Science, Technology, Sports and Culture of Japan. The authors have no conflicting financial interests. Funding to pay the Open Access publication charge was provided by a grant from the Ministry of Health, Labor, and Welfare of Japan.

Conflict of interest statement. None declared.

REFERENCES

1. Sheehy,A.M., Gaddis,N.C., Choi,J.D. and Malim,M.H. (2002) Isolation of a human gene that inhibits HIV-1 infection and is suppressed by the viral Vif protein. *Nature*, **418**, 646–650.
2. Harris,R.S., Bishop,K.N., Sheehy,A.M., Craig,H.M., Petersen-Mahrt,S.K., Watt,I.N., Neuberger,M.S. and Malim,M.H. (2003) DNA deamination mediates innate immunity to retroviral infection. *Cell*, **113**, 803–809.
3. Mangeat,B., Turelli,P., Caron,G., Friedli,M., Perrin,L. and Trono,D. (2003) Broad antiretroviral defence by human APOBEC3G through lethal editing of nascent reverse transcripts. *Nature*, **424**, 99–103.
4. Zhang,H., Yang,B., Pomerantz,R.J., Zhang,C., Arunachalam,S.C. and Gao,L. (2003) The cytidine deaminase CEM15 induces hypermutation in newly synthesized HIV-1 DNA. *Nature*, **424**, 94–98.
5. Mariani,R., Chen,D., Schrofelbauer,B., Navarro,F., Konig,R., Bollman,B., Munk,C., Nymark-McMahon,H. and Landau,N.R. (2003) Species-specific exclusion of APOBEC3G from HIV-1 virions by Vif. *Cell*, **114**, 21–31.
6. Bogerd,H.P., Doehle,B.P., Wiegand,H.L. and Cullen,B.R. (2004) A single amino acid difference in the host APOBEC3G protein controls the primate species specificity of HIV type 1 virion infectivity factor. *Proc. Natl Acad. Sci. USA*, **101**, 3770–3774.
7. Mangeat,B., Turelli,P., Liao,S. and Trono,D. (2004) A single amino acid determinant governs the species-specific sensitivity of APOBEC3G to Vif action. *J. Biol. Chem.*, **279**, 14481–14483.
8. Schrofelbauer,B., Chen,D. and Landau,N.R. (2004) A single amino acid of APOBEC3G controls its species-specific interaction with virion infectivity factor (Vif). *Proc. Natl Acad. Sci. USA*, **101**, 3927–3932.
9. Russell,R.A., Wiegand,H.L., Moore,M.D., Schafer,A., McClure,M.O. and Cullen,B.R. (2005) Foamy virus Bet proteins function as novel inhibitors of the APOBEC3 family of innate antiretroviral defense factors. *J. Virol.*, **79**, 8724–8731.
10. Delebecque,F., Suspene,R., Calattini,S., Casartelli,N., Saib,A., Froment,A., Wain-Hobson,S., Gessain,A., Vartanian,J.P. *et al.* (2006) Restriction of foamy viruses by APOBEC cytidine deaminases. *J. Virol.*, **80**, 605–614.
11. Sasada,A., Takaori-Kondo,A., Shirakawa,K., Kobayashi,M., Abudu,A., Hishizawa,M., Imada,K., Tanaka,Y. and Uchiyama,T. (2005) APOBEC3G targets human T-cell leukemia virus type 1. *Retrovirology*, **2**, 32.
12. Kobayashi,M., Takaori-Kondo,A., Shindo,K., Abudu,A., Fukunaga,K. and Uchiyama,T. (2004) APOBEC3G targets specific virus species. *J. Virol.*, **78**, 8238–8244.
13. Turelli,P., Mangeat,B., Jost,S., Vianin,S. and Trono,D. (2004) Inhibition of hepatitis B virus replication by APOBEC3G. *Science*, **303**, 1829.
14. Noguchi,C., Ishino,H., Tsuge,M., Fujimoto,Y., Imamura,M., Takahashi,S. and Chayama,K. (2005) G to A hypermutation of hepatitis B virus. *Hepatology*, **41**, 626–633.
15. Esnault,C., Heidmann,O., Delebecque,F., Dewannieux,M., Ribet,D., Hance,A.J., Heidmann,T. and Schwartz,O. (2005)

APOBEC3G cytidine deaminase inhibits retrotransposition of endogenous retroviruses. *Nature*, **433**, 430–433.
16. Macduff,D.A. and Harris,R.S. (2006) Directed DNA deamination by AID/APOBEC3 in immunity. *Curr. Biol.*, **16**, R186–R189.
17. OhAinle,M., Kerns,J.A., Malik,H.S. and Emerman,M. (2006) Adaptive evolution and antiviral activity of the conserved mammalian cytidine deaminase APOBEC3H. *J. Virol.*, **80**, 3853–3862.
18. Sawyer,S.L., Emerman,M. and Malik,H.S. (2004) Ancient adaptive evolution of the primate antiviral DNA-editing enzyme APOBEC3G. *PLoS Biol.*, **2**, E275.
19. Lander,E.S., Linton,L.M., Birren,B., Nusbaum,C., Zody,M.C., Baldwin,J., Devon,K., Dewar,K., Doyle,M. *et al.* (2001) Initial sequencing and analysis of the human genome. *Nature*, **409**, 860–921.
20. Sassaman,D.M., Dombroski,B.A., Moran,J.V., Kimberland,M.L., Naas,T.P., DeBerardinis,R.J., Gabriel,A., Swergold,G.D. and Kazazian,H.H.Jr (1997) Many human L1 elements are capable of retrotransposition. *Nat. Genet.*, **16**, 37–43.
21. Brouha,B., Schustak,J., Badge,R.M., Lutz-Prigge,S., Farley,A.H., Moran,J.V. and Kazazian,H.H.Jr (2003) Hot L1s account for the bulk of retrotransposition in the human population. *Proc. Natl Acad. Sci. USA*, **100**, 5280–5285.
22. Dombroski,B.A., Mathias,S.L., Nanthakumar,E., Scott,A.F. and Kazazian,H.H.Jr (1991) Isolation of an active human transposable element. *Science*, **254**, 1805–1808.
23. Kolosha,V.O. and Martin,S.L. (2003) High-affinity, non-sequence-specific RNA binding by the open reading frame 1 (ORF1) protein from long interspersed nuclear element 1 (LINE-1). *J. Biol. Chem.*, **278**, 8112–8117.
24. Feng,Q., Moran,J.V., Kazazian,H.H.Jr and Boeke,J.D. (1996) Human L1 retrotransposon encodes a conserved endonuclease required for retrotransposition. *Cell*, **87**, 905–916.
25. Mathias,S.L., Scott,A.F., Kazazian,H.H.Jr, Boeke,J.D. and Gabriel,A. (1991) Reverse transcriptase encoded by a human transposable element. *Science*, **254**, 1808–1810.
26. Dombroski,B.A., Feng,Q., Mathias,S.L., Sassaman,D.M., Scott,A.F., Kazazian,H.H.Jr and Boeke,J.D. (1994) An in vivo assay for the reverse transcriptase of human retrotransposon L1 in Saccharomyces cerevisiae. *Mol. Cell. Biol.*, **14**, 4485–4492.
27. Kazazian,H.H.Jr, Wong,C., Youssoufian,H., Scott,A.F., Phillips,D.G. and Antonarakis,S.E. (1988) Haemophilia A resulting from de novo insertion of L1 sequences represents a novel mechanism for mutation in man. *Nature*, **332**, 164–166.
28. Woods-Samuels,P., Wong,C., Mathias,S.L., Scott,A.F., Kazazian,H.H.Jr and Antonarakis,S.E. (1989) Characterization of a nondeleterious L1 insertion in an intron of the human factor VIII gene and further evidence of open reading frames in functional L1 elements. *Genomics*, **4**, 290–296.
29. Li,X., Scaringe,W.A., Hill,K.A., Roberts,S., Mengos,A., Careri,D., Pinto,M.T., Kasper,C.K. and Sommer,S.S. (2001) Frequency of recent retrotransposition events in the human factor IX gene. *Hum. Mutat.*, **17**, 511–519.
30. Narita,N., Nishio,H., Kitoh,Y., Ishikawa,Y., Ishikawa,Y., Minami,R., Nakamura,H. and Matsuo,M. (1993) Insertion of a 5' truncated L1 element into the 3' end of exon 44 of the dystrophin gene resulted in skipping of the exon during splicing in a case of Duchenne muscular dystrophy. *J. Clin. Invest.*, **91**, 1862–1867.
31. Holmes,S.E., Dombroski,B.A., Krebs,C.M., Boehm,C.D. and Kazazian,H.H.Jr (1994) A new retrotransposable human L1 element from the LRE2 locus on chromosome 1q produces a chimaeric insertion. *Nat. Genet.*, **7**, 143–148.
32. Yoshida,K., Nakamura,A., Yazaki,M., Ikeda,S. and Takeda,S. (1998) Insertional mutation by transposable element, L1, in the DMD gene results in X-linked dilated cardiomyopathy. *Hum. Mol. Genet.*, **7**, 1129–1132.
33. Kazazian,H.H.Jr (1998) Mobile elements and disease. *Curr. Opin. Genet. Dev.*, **8**, 343–350.
34. Meischl,C., Boer,M., Ahlin,A. and Roos,D. (2000) A new exon created by intronic insertion of a rearranged LINE-1 element as the cause of chronic granulomatous disease. *Eur. J. Hum. Genet.*, **8**, 697–703.
35. Schwahn,U., Lenzner,S., Dong,J., Feil,S., Hinzmann,B., van Duijnhoven,G., Kirschner,R., Hemberger,M., Bergen,A.A. *et al.* (1998) Positional cloning of the gene for X-linked retinitis pigmentosa 2. *Nat. Genet.*, **19**, 327–332.
36. Miki,Y., Nishisho,I., Horii,A., Miyoshi,Y., Utsunomiya,J., Kinzler,K.W., Vogelstein,B. and Nakamura,Y. (1992) Disruption of the APC gene by a retrotransposal insertion of L1 sequence in a colon cancer. *Cancer Res.*, **52**, 643–645.
37. Gilbert,N., Lutz-Prigge,S. and Moran,J.V. (2002) Genomic deletions created upon LINE-1 retrotransposition. *Cell*, **110**, 315–325.
38. Prak,E.T., Dodson,A.W., Farkash,E.A. and Kazazian,H.H.Jr (2003) Tracking an embryonic L1 retrotransposition event. *Proc. Natl Acad. Sci. USA*, **100**, 1832–1837.
39. Zheng,Y.H., Irwin,D., Kurosu,T., Tokunaga,K., Sata,T. and Peterlin,B.M. (2004) Human APOBEC3F is another host factor that blocks human immunodeficiency virus type 1 replication. *J. Virol.*, **78**, 6073–6076.
40. Kinomoto,M., Yokoyama,M., Sato,H., Kojima,A., Kurata,T., Ikuta,K., Sata,T. and Tokunaga,K. (2005) Amino acid 36 in the human immunodeficiency virus type 1 gp41 ectodomain controls fusogenic activity: implications for the molecular mechanism of viral escape from a fusion inhibitor. *J. Virol.*, **79**, 5996–6004.
41. Tachiwana,H., Shimura,M., Nakai-Murakami,C., Tokunaga,K., Takizawa,Y., Sata,T., Kurumizaka,H. and Ishizaka,Y. (2006) HIV-1 Vpr induces DNA double-strand breaks. *Cancer Res.*, **66**, 627–631.
42. Ono,T., Isobe,K., Nakada,K. and Hayashi,J.I. (2001) Human cells are protected from mitochondrial dysfunction by complementation of DNA products in fused mitochondria. *Nat. Genet.*, **28**, 272–275.
43. Fouchier,R.A., Meyer,B.E., Simon,J.H., Fischer,U. and Malim,M.H. (1997) HIV-1 infection of non-dividing cells: evidence that the amino-terminal basic region of the viral matrix protein is important for Gag processing but not for post-entry nuclear import. *EMBO J.*, **16**, 4531–4539.
44. Gorlich,D. and Kutay,U. (1999) Transport between the cell nucleus and the cytoplasm. *Annu. Rev. Cell Dev. Biol.*, **15**, 607–660.
45. Bogerd,H.P., Wiegand,H.L., Hulme,A.E., Garcia-Perez,J.L., O'Shea,K.S., Moran,J.V. and Cullen,B.R. (2006) Cellular inhibitors of long interspersed element 1 and Alu retrotransposition. *Proc. Natl Acad. Sci. USA*, **103**, 8780–8785.
46. Wiegand,H.L., Doehle,B.P., Bogerd,H.P. and Cullen,B.R. (2004) A second human antiretroviral factor, APOBEC3F, is suppressed by the HIV-1 and HIV-2 Vif proteins. *EMBO J.*, **23**, 2451–2458.
47. Yu,Q., Chen,D., Konig,R., Mariani,R., Unutmaz,D. and Landau,N.R. (2004) APOBEC3B and APOBEC3C are potent inhibitors of simian immunodeficiency virus replication. *J. Biol. Chem.*, **279**, 53379–53386.
48. Doehle,B.P., Schafer,A. and Cullen,B.R. (2005) Human APOBEC3B is a potent inhibitor of HIV-1 infectivity and is resistant to HIV-1 Vif. *Virology*, **339**, 281–288.
49. Dang,Y., Wang,X., Esselman,W.J. and Zheng,Y.H. (2006) Identification of APOBEC3DE as another antiretroviral factor from the human APOBEC family. *J. Virol*, **80**, 10522–10533.
50. Langlois,M.A., Beale,R.C., Conticello,S.G. and Neuberger,M.S. (2005) Mutational comparison of the single-domained APOBEC3C and double-domained APOBEC3F/G anti-retroviral cytidine deaminases provides insight into their DNA target site specificities. *Nucleic Acids Res.*, **33**, 1913–1923.
51. Liddament,M.T., Brown,W.L., Schumacher,A.J. and Harris,R.S. (2004) APOBEC3F properties and hypermutation preferences indicate activity against HIV-1 in vivo. *Curr. Biol.*, **14**, 1385–1391.
52. Bogerd,H.P., Wiegand,H.L., Doehle,B.P., Lueders,K.K. and Cullen,B.R. (2006) APOBEC3A and APOBEC3B are potent inhibitors of LTR-retrotransposon function in human cells. *Nucleic Acids Res.*, **34**, 89–95.
53. Muckenfuss,H., Hamdorf,M., Held,U., Perkovic,M., Lower,J., Cichutek,K., Flory,E., Schumann,G.G. and Munk,C. (2006) APOBEC3 proteins inhibit human LINE-1 retrotransposition. *J. Biol. Chem.*, **281**, 22161–22172.
54. Stenglein,M.D. and Harris,R.S. (2006) APOBEC3B and APOBEC3F inhibit L1 retrotransposition by a DNA deamination-independent mechanism. *J. Biol. Chem.*, **281**, 16837–16841.
55. Chen,H., Lilley,C.E., Yu,Q., Lee,D.V., Chou,J., Narvaiza,I., Landau,N.R. and Weitzman,M.D. (2006) APOBEC3A is a potent inhibitor of adeno-associated virus and retrotransposons. *Curr. Biol.*, **16**, 480–485.

56. Turelli,P., Vianin,S. and Trono,D. (2004) The innate antiretroviral factor APOBEC3G does not affect human LINE-1 retrotransposition in a cell culture assay. *J. Biol. Chem.*, **279**, 43371–43373.
57. Chiu,Y.L., Soros,V.B., Kreisberg,J.F., Stopak,K., Yonemoto,W. and Greene,W.C. (2005) Cellular APOBEC3G restricts HIV-1 infection in resting CD4+ T cells. *Nature*, **435**, 108–114.
58. Esnault,C., Millet,J., Schwartz,O. and Heidmann,T. (2006) Dual inhibitory effects of APOBEC family proteins on retrotransposition of mammalian endogenous retroviruses. *Nucleic Acids Res.*, **34**, 1522–1531.
59. Newman,E.N., Holmes,R.K., Craig,H.M., Klein,K.C., Lingappa,J.R., Malim,M.H. and Sheehy,A.M. (2005) Antiviral function of APOBEC3G can be dissociated from cytidine deaminase activity. *Curr. Biol.*, **15**, 166–170.
60. Bishop,K.N., Holmes,R.K. and Malim,M.H. (2006) Antiviral potency of APOBEC proteins does not correlate with cytidine deamination. *J. Virol.*, **80**, 8450–8458.
61. Guo,F., Cen,S., Niu,M., Saadatmand,J. and Kleiman,L. (2006) Inhibition of formula-primed reverse transcription by human APOBEC3G during human immunodeficiency virus type 1 replication. *J. Virol.*, **80**, 11710–11722.
62. Cost,G.J., Feng,Q., Jacquier,A. and Boeke,J.D. (2002) Human L1 element target-primed reverse transcription in vitro. *EMBO J.*, **21**, 5899–5910.
63. Hohjoh,H. and Singer,M.F. (1996) Cytoplasmic ribonucleoprotein complexes containing human LINE-1 protein and RNA. *EMBO J.*, **15**, 630–639.
64. Hohjoh,H. and Singer,M.F. (1997) Sequence-specific single-strand RNA binding protein encoded by the human LINE-1 retrotransposon. *EMBO J.*, **16**, 6034–6043.
65. Esnault,C., Maestre,J. and Heidmann,T. (2000) Human LINE retrotransposons generate processed pseudogenes. *Nat. Genet.*, **24**, 363–367.
66. Wei,W., Gilbert,N., Ooi,S.L., Lawler,J.F., Ostertag,E.M., Kazazian,H.H., Boeke,J.D. and Moran,J.V. (2001) Human L1 retrotransposition: cis preference versus trans complementation. *Mol. Cell. Biol.*, **21**, 1429–1439.
67. Yu,Q., Konig,R., Pillai,S., Chiles,K., Kearney,M., Palmer,S., Richman,D., Coffin,J.M. and Landau,N.R. (2004) Single-strand specificity of APOBEC3G accounts for minus-strand deamination of the HIV genome. *Nat. Struct. Mol. Biol.*, **11**, 435–442.
68. Goodier,J.L., Ostertag,E.M., Engleka,K.A., Seleme,M.C. and Kazazian,H.H.Jr (2004) A potential role for the nucleolus in L1 retrotransposition. *Hum. Mol. Genet.*, **13**, 1041–1048.
69. Kubo,S., Seleme Mdel,C., Soifer,H.S., Perez,J.L., Moran,J.V., Kazazian,H.H.Jr and Kasahara,N. (2006) L1 retrotransposition in nondividing and primary human somatic cells. *Proc. Natl Acad. Sci. USA*, **103**, 8036–8041.
70. Nelson-Rees,W.A., Hunter,L., Darlington,G.J. and O'Brien,S.J. (1980) Characteristics of HeLa strains: permanent vs. variable features. *Cytogenet. Cell Genet.*, **27**, 216–231.
71. Bishop,K.N., Holmes,R.K., Sheehy,A.M., Davidson,N.O., Cho,S.J. and Malim,M.H. (2004) Cytidine deamination of retroviral DNA by diverse APOBEC proteins. *Curr. Biol.*, **14**, 1392–1396.

AIDS RESEARCH AND HUMAN RETROVIRUSES
Volume 23, Number 3, 2007, pp. 000–000

DOI: 10.1089/aid.2006.0124

Vpr in Plasma of HIV Type 1-Positive Patients Is Correlated with the HIV Type 1 RNA Titers

SHIGEKI HOSHINO,[1,2] BINLIAN SUN,[1] MITSURU KONISHI,[3] MARI SHIMURA,[1] TATSUYA SEGAWA,[4] YOSHIAKI HAGIWARA,[4] YOSHIO KOYANAGI,[5] AIKICHI IWAMOTO,[6] JUN-ICHI MIMAYA,[7] HIROSHI TERUNUMA,[8] SHIGEYUKI KANO,[1,2] and YUKIHITO ISHIZAKA[1]

ABSTRACT

Vpr, an accessory gene product of HIV-1, has been reported in the plasma of HIV-1-positive patients, and exogenous Vpr induces the reactivation of viral production from latently infected cells and the apoptosis of T cells *in vitro*. These observations imply that Vpr is important in AIDS development, but the clinical relevance of the findings cannot be evaluated fully because the actual plasma Vpr concentration in HIV-1-positive patients is unknown. Here we generated two monoclonal antibodies against different portions of Vpr and successfully identified Vpr as a 14-kDa protein in HIV-1-positive patients. Semiquantitative analysis using a recombinant Vpr revealed that the concentration of Vpr in patient plasma was ~0.6 nM (10 ng/ml). Cross-sectional analysis of 52 HIV-1-positive patients revealed that the presence of Vpr detected in 20 patients was positively correlated with HIV-1 RNA copy number ($p < 0.03$), but not with the number of CD4$^+$ T cells. This is the first report demonstrating the actual amount of Vpr in HIV-1-positive patients, and the possible linkage of Vpr and viral titers indicates it is important to continue to carry out the sequential analysis of Vpr, especially in clinical courses of HIV-1-positive patients. The threshold of viral titers, where Vpr appears in the patients' plasma, if present, contributes to better understanding the role of Vpr in AIDS pathogenesis.

THE ADOPTION OF ANTIRETROVIRAL THERAPY (ART) has improved the prognosis of HIV-1-positive patients.[1] However, the complete elimination of the virus from patients receiving ART is estimated to take more than 60 years.[2] One factor that may be responsible for this problem is that HIV-1 infects macrophages, latent viral reservoirs[3] from which recurrent viral production is induced by various factors.[4] *Vpr*, an accessory gene of HIV-1, encodes a virion-associated 14-kDa protein that may be critical for the primary infection of macrophages.[5–7] Vpr also induces the reactivation of viral reproduction from latently infected cells. The presence of Vpr in the sera of HIV-1-positive patients, along with the induction of viral reproduction by exogenous Vpr,[8,9] implies that Vpr is actively involved in AIDS development. However, it is necessary to determine the concentration of Vpr in patient plasma samples to correctly evaluate the clinical significance of data obtained from *in vitro* experiments. In the current study, we successfully detected Vpr in patients' samples.

The protocol of this study was approved by the ethics committees of the International Medical Centre of Japan, Nara University School of Medicine, Shizuoka Children's Hospital, and five other hospitals in collaboration with Shizuoka Children's Hospital. Blood plasma samples and peripheral blood were obtained from patients who had given informed consent after the experiment was explained to them. Clinical data on 14 outpatients at Nara University School of Medicine, who were en-

[1]Research Institute, International Medical Center of Japan, Shinjuku-ku, Tokyo 162-8655, Japan.
[2]Graduate School of Comprehensive Human Sciences, University of Tsukuba, Tsukuba 305-8577, Japan.
[3]Center for Infectious Diseases, Nara Medical University, Kashihara, Nara 634-8522, Japan
[4]Immuno-Biological Laboratories, Co., Fujioka, Gunma 375-0005, Japan.
[5]Laboratory of Viral Pathogenesis, Institute for Virus Research, Kyoto University, Sakyou-ku, Kyoto 606-8507, Japan.
[6]Department of Infectious Diseases, The Institute of Medical Science, The University of Tokyo, Minato-ku 108-8639, Tokyo, Japan.
[7]Department of Hematology and Oncology, Children's Hospital of Shizuoka Prefecture, Aoi-ku, Shizuoka 420-8660, Japan.
[8]Biotherapy Institute of Japan, Koutou-ku, Tokyo, 135-0051.

T1 rolled in the initial study, are summarized in Table 1. For the second study, samples from an additional 38 patients were analyzed. The median numbers of HIV-1 RNA copies (32,289.3 copies/ml), $CD4^+$ T cells (449.4 copies/ml), and total white blood cells (5049.0 cells/ml) were determined in all 52 patients. Control healthy plasma samples were obtained from Teragenix Corporation (Kokusai Bio, Tokyo). A recombinant Vpr protein (rVpr) was first prepared as a fusion protein with glutathione *S*-transferase (GST) expressed by pGEX6-P-1, and purified according to the manufacturer's protocol (GE Healthcare Bio-Sciences, Piscataway, NJ). The purified rVpr appeared as a single band on Coomassie brilliant blue staining (supplementary information 1a: SI-1a). Two mouse monoclonal antibodies, 8D1 (IgG2a) and C217 (IgG2b), were generated by immunization with a full-length Vpr peptide, chemically synthesized based on the prototype NL4-3[10] (Osaka Peptide Institute, Osaka), and a synthetic peptide encompassing its carboxy (C)-terminal region (Wako Pure Chemical Industries, Tokyo, Japan), respectively. An enzyme-linked immunosorbent assay (ELISA) was based on 8D1, as the primary antibody, and a purified rabbit IgG antibody, raised against the peptide of the C-terminal 18 amino acids of Vpr (IBL, Fujioka, Japan), as the second antibody. Although the Vpr-ELISA could clearly detect purified rVpr (SI-1b), we found that the system occasionally detected one or more cross-reacting peptide in healthy persons (data not shown). Therefore, we decided to carry out a semiquantitative analysis using immunoprecipitation-Western blotting (IP-WB) analysis, with rVpr quantified by ELISA as the standard. For the IP-WB analysis, 0.5 mg of C217 was bound to Protein G Sepharose (GE Healthcare Bio-Sciences). Each 200 μl of plasma was first treated with DNase I and RNase A for 5 min, and then incubated with 10 μl of C217-coupled beads for 2 h at 4°C. After being washed in buffer with 0.05% Tween-20, the immunoprecipitate was subjected to Western blot analysis. For standard samples, different amounts of purified rVpr were added to 200 μl of control plasma. No detergents were added when the samples were incubated with the primary antibody, so that the IP-WB would detect only soluble Vpr, and not Vpr in viral particles.[10] The detection limit of the system was about 1 ng/ml (0.07 nM) (SI-2a).

Representative results from the IP-WB analysis of 14 plasma samples are shown in Fig. 1a. A definite signal of the 14-kDa protein was observed in patients N-09, 11, and 13 (Fig. 1a). By contrast, no peptides around 14 kDa were detected in more than 60 specimens from healthy volunteers (Fig. 1b). Because the IP-WB could selectively detect the 14-kDa peptide in the culture supernatant of cells containing an expression plasmid encoding *vpr* (SI-2b), we concluded that Vpr was the 14-kDa peptide detected by the IP–WB. A comparison of the signal intensities of the detected bands and standard rVpr (Fig. 1a; 5, 2.5, and 1.25 μg/ml signals, and N-11) indicated that the serum Vpr concentration was about 0.4 nM. F1

During the analysis, we did not detect the Vpr signal in one patient (N-10; Table 1) who had 11,000 copies/ml of HIV-1 RNA (Fig. 1a, lower panel). To evaluate whether our system failed to detect Vpr mutants differing from the prototype NL4-3 (GenBank accession number M19921), we amplified DNA fragments from peripheral blood mononuclear cells covering the entire *vpr* gene. Then we determined its nucleotide sequence (Fig. 2a, and primers in SI-3). The deduced amino acid sequences are also shown in Fig. 2b. Interestingly, the *vpr* gene from patient N-10 had a four-nucleotide (TTAA) insertion at nucleotide 81, designated "clone 10," which generates a frameshift mutation within the inserted sequence (shown by the F2

TABLE 1. CLINICAL DATA OF PATIENTS SUBJECTED TO ANALYSIS AND RESULTS OF THE IP-WB

						Clinical data				
						White blood cells (/mm³)				
Case number	*Sex*	*Age*	*Causes of infection*	*Conditions*	*Treatment status*[1]	*Total number*	*Lymphocytes*	*$CD4^+$ T cells*	*HIV-1 RNA (copies/ml)*	*Vpr*[2]
N-01	M	39	HO[3]	AIDS[4]	2	8400	2612	771	<50	−
02	M	41	HO	AIDS	2	6800	2584	346	<50	−
03	M	59	HE[3]	AIDS	2	4700	2444	381	260	−
04	F	32	HE	AC[4]	3	6300	1890	302	4,400	−
05	M	38	HO	AIDS	2	8600	2417	585	<50	−
06	M	35	HO	AC	1	4900	1274	116	220,000	+++
07	M	45	BL[3]	AIDS	2	2600	546	38	73,000	++
08	M	58	HE	AIDS	2	6800	1632	366	<50	−
09	M	29	BL	AC	1	3000	1056	266	17,000	+
10	M	23	HO	AC	1	5200	1300	230	11,000	−
11	F	37	HE	AC	1	4600	1150	222	500,000	+++
12	F	40	HE	AC	1	6600	1584	598	98	−
13	M	42	BL	AIDS	2	3100	1054	110	70,000	++
14	M	23	HO	AC	1	5800	2656	553	71,000	++

[1]Group 1, no therapy; group 2, under medication; group 3, posttherapy.
[2]Based on results of the IP-WB, patients are divided into four groups; Vpr-negative (−) and Vpr-positive with less than 1 ng/ml (+), with 1–5 ng/ml (++), and with more than 5 ng/ml (+++).
[3]HO, homosexual; HE, heterosexual; BL, blood products.
[4]AIDS, acquired immunodeficiency syndrome; AC, asymtomatic carrier.

QU1

box in Fig. 2a). However, because this patient had no deletion in the 3′ region of the *vpr* gene, it was possible to clone the gene. Repeated sequence analyses of several clones of the amplified *vpr* DNA indicated that clone 10 was the major *vpr* in this patient (SI-4). The negative results of the IP-WB analysis for patient N-10 were therefore due to truncation of the C-terminal region.

Additional sequence analysis revealed that "clone N (Nara)," which differs by four amino acids from the prototype NL4-3 (Fig. 2b), was frequently observed in the analyzed patients (patients N-04, 05, 08, 09, 11, and 12). Interestingly, although patient N-09 had clone N as a major variant—all seven clones sequenced from the PCR products were identified as clone N (see SI-4)—the IP-WB analysis (Fig. 1a, lower panel) detected a positive Vpr signal in patient N-09. This suggests that C217 antibody, which was used as the first antibody in immunoprecipitation, reacts with the protein encoded by clone N, even though its C-terminal region differs from the prototype NL4-3 clone by two amino acids (Fig. 2b).

Next, we examined the possible correlation of Vpr and clinical manifestations. An analysis of 14 patients suggested a positive link between Vpr and viral titers (data not shown). To examine this possibility, we analyzed an additional 38 stocked samples using IP-WB. We detected Vpr in 14 samples. A representative result of the second analysis is shown in Fig. 1c. Positive Vpr signals were detected in patients T-166, 167, and 175. Then we examined the relationship between Vpr and RNA copy number. As shown in Fig. 3a, we found a positive correlation between the detection of Vpr and RNA copy number ($p < 0.03$). In contrast, we did not detect a positive relationship between Vpr and the numbers of $CD4^+$ T cells or total white blood cells. The distribution of Vpr-positive patients based on the concentration of Vpr implied that the amount of Vpr in plasma samples is correlated with HIV-1 RNA copy numbers (Fig. 3b).

In the current work, we successfully identified Vpr in 22 samples from 52 HIV-1-positive patients. A comparison of the signals obtained with standard rVpr revealed that the Vpr concentration was ~0.4 nM. Levy *et al.*[9] suggested that Vpr is present in patient plasma, with rVpr activating viral reproduction when added to the culture medium of latently infected cells. In addition, Muthumani *et al.* proposed that exogenous rVpr has various activities, such as inducing T cell apoptosis,[11] inhibiting macrophage function,[12] and suppressing NF-κB signaling.[13] However, these experiments did not consider the actual amount of Vpr present in the plasma samples. Our result is the first demonstration of Vpr in HIV-1-positive patients, and provides a rationale for the dose of rVpr suitable for *in vitro* experiments.

We observed a good correlation between the detection of Vpr and HIV-1 RNA copy number ($p < 0.03$) (Fig. 3a). It has been reported that the exogenous Vpr induces viral production from latently infected cells, implying that Vpr is involved in viral reproduction *in vivo*. An important question still to be answered is how the Vpr titer changes in the context of viral replication during the clinical course of the disease. It is important to clarify whether Vpr functions as an initial trigger of viral expansion *in vivo*.

We did not detect a link between Vpr and the numbers of $CD4^+$ T cells. Recently, it was determined that WT-Vpr and its variant R77Q act differently in modifying the clinical features of HIV-1-positive patients. Based on several reports, it has been proposed that R77Q is a candidate marker for long-term nonprogression (LTNP),[14–16] although this is still controversial.[17,18] In this study, we observed that the main Vpr variants of patients N-04, 09, and 10 were R77Q or C-terminally truncated. However, we did not recognize these patients as candidates for LTNP (clinical observation by M. Konishi). The involvement of WT-Vpr and R77Q in patients is rationalized by *in vitro* experiments showing that rVpr induces the apoptosis of $CD4^+$ T cells.[11,12,14,15] whereas R77Q has less potent apoptosis activity than WT-Vpr.[15] It is important to note that the *in vitro* studies of the differential activities of exogenous WT-Vpr and R77Q used tremendous amounts of the proteins, and a difference in activity was observed only when 1.5–2.0 μM of the peptides was used.[15] As shown here, the concentration of Vpr in patient plasma was a maximum of 1.0 nM, and it is crucial to compare the functional difference of these molecules at a concentration comparable to that observed *in vivo*. Careful studies are required to address this matter.

SUPPLEMENTARY INFORMATION

SI-1. Purification of rVpr and measurement using ELISA. (**a**) Expression and purification profiles of rVpr. Vpr was expressed as a fusion protein with GST and purified in a glutathione column. Lane 1, marker; lane 2, initial lysate; lane 3, flow-through sample eluted from the glutathione column; lane 4, eluate from rVpr after treatment with precision protease; and lane 5, eluate from an affinity column containing a monoclonal antibody against Vpr (8D1). The arrowhead and arrow indicate the position of GST-Vpr and purified rVpr, respectively. Proteins were stained with Coomassie brilliant blue solution. (**b**) ELISA verion-1 for measuring rVpr. Synthesized full-length Vpr was used to make a standard curve. To the Vpr-ELISA were added 10 ng/ml each of GAPDH, HIV-1 integrase, and SARS-CoV Spike protein, which were expressed as a (His)-tagged protein, and purified using Ni-beads. Note that none of the samples gave cross-signals with Vpr. The amount of rVpr was assessed using the absorbance at OD450 nm, as shown with the dotted line.

SI-2. Detection of Vpr by the IP-WB. (**a**) Sensitivity of the system. The IP-WB analysis was conducted using C217 for IP and 8D1 for WB. To determine the sensitivity of the system, 10, 5, 2.5, and 1.25 ng of purified rVpr were added to 200 μl of plasma from a healthy human just before the IP-WB analysis. The signals obtained using IP-WB (upper panel) and the input rVpr (lower panel) detected by 8D1 are shown. (**b**) Detection of Vpr in a culture supernatant. Culture supernatants (sup.) of 293FS cells (Invitrogen) transfected with pcDNA3.1 (center lane, "Vec") or pcDNA3.1-*vpr* (right lane, "Vpr") were collected on day 6 after transfection, and the IP-WB analysis was carried out. The rVpr (400 pg/lane) was included in the same blot as a positive control of WB (left lane).

SI-3. Cloning and sequence analysis of *vpr*. DNA covering *vpr* was amplified from the genomic DNA of peripheral blood cells using nested PCR. The primers used were Vpr1F (nt 4713–4733, 5′-GACCCTGACCTAGCAGACCA-3′) and Vpr1R (nt 5298–5318, 5′-CAAACTTGGCAATGAAAGCA-3′) for the first

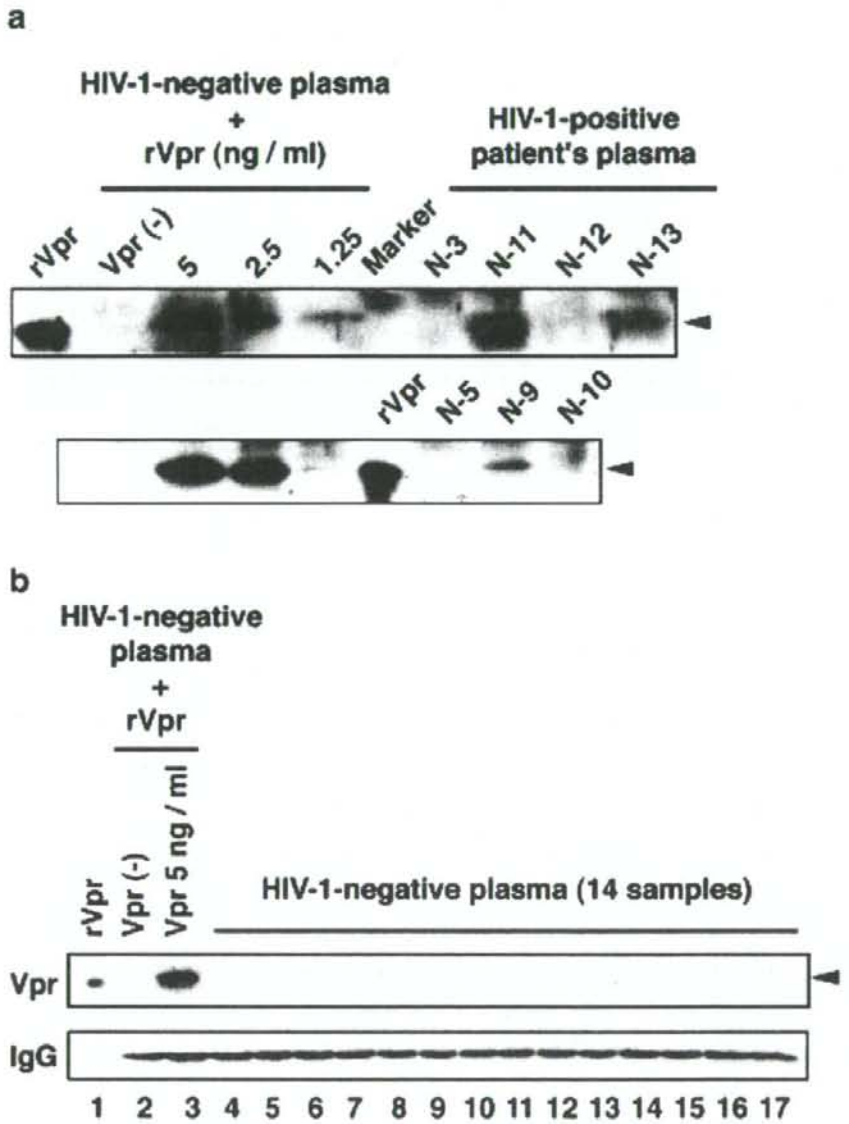

FIG. 1. Detection of Vpr in sera of HIV-1-positive patients. (**a**) Presence of the 14-kDa Vpr protein in HIV-1-positive patients. To semiquantify the Vpr concentration in patient samples, 5, 2.5, and 1.25 ng of standard rVpr (lanes 2–5), which had been measured using ELISA version-1 (see supplementary information 1b; SI-1b), were included. As a positive control for the WB analysis, 1 ng of rVpr (lane 1) was also included. Signals of HIV-1-positive plasma (lanes 7–10) and a molecular marker (lane 6) are shown. (**b**) Representative results of the IP-WB analysis of healthy volunteers. The IP-WB analysis was performed on more than 60 samples from healthy volunteers, and representative results from 14 cases (lanes 4–17) are shown. Note that no signals were detected around 14 kDa. The results for input rVpr (lane 1), no rVpr (lane 2), or 5 ng Vpr (lane 3) added to normal plasma are shown. IgG signals recovered after IP are also shown (lower panel). (**c**) Detection of the 14-kDa Vpr protein in HIV-1-positive patients in the second group. Also in this analysis, 5, 2.5, and 1.25 ng of standard rVpr (lanes 2–5) were included to assess the concentration of Vpr in patient plasma samples.

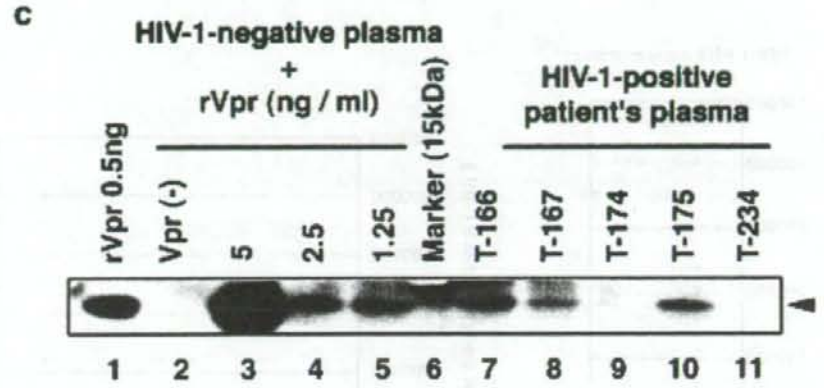

FIG. 1. (*Continued*).

PCR. For the second PCR, Vpr2F (nt. 4854–4875, 5′-CAGTACTTGGCACTAGCAGCA-3′) and Vpr2R (nt 5243–5263, 5′-TAGGCTGACTTCCTGGATGC-3′) were used (GenBank accession number M19921). The first and second rounds of PCR were performed for 30 cycles of 95°C for 30 sec, 62°C for 30 sec, and 72°C for 1 min and for 95°C for 30 sec, 64°C for 30 sec, and 72°C for 45 sec, respectively. The PCR products were cloned into pZero Blunt topo vector (Invitrogen, Carlsbad, CA). Several clones were sequenced for each PCR product.

SI-4. See Table 2.

T2

a

```
NL4-3     1 ATGGAACAAG CCCCAGAAGA CCAAGGGCCA CAGAGGGAGC CATACAACGA ATGGACACTA
Clone-10  1 ---------- ---------- ---------- ---------- ---------- ----------

         61 GAGCTTTTAG AGGAACTTAA    GAGTGA AGCTGTTAGA CATTTTCCTA GGATATGGCT
         61 ---------- ---------- TTAA------ ---------- ---------- ----------

        117 CCATAACTTA GGACGACATA TCTATGAAAC TTACGGGGAT ACTTGGGCAG GAGTGGAAGC
        121 ---------- ---------- ---------- ---------- ---------- ----------

        177 CATAATAAGA ATTCTGCAAC AACTGCCGTT TATCCATTTC AGAATTGGGT GTCGACATAG
        181 ---------- ---------- ---------- ---------- ---------- ----------

        237 CAGAATAGGC GTTACTCGAC AGAGGAGAGC AAGAAATGGA GCCAGTAG 284nt.
        241 ---------- ---------- ---------- ---------- -------- 288nt.
```

b

```
NL4-3     MEQAPEDQGPQREPYNEWTLELLEELKSEAVRHFPRIWLHNLGQHIYETYGDTWAGVEAIIRILQQLPFIHFRIGCRHSRIGVTRQRRARNGASRS
Clone-10  ·························N*
Clone-N   ·····························································L·····Q····II···········
Mutant-1  ·····························································L··························
```

FIG. 2. Sequence analysis of *vprs* and the deduced amino acids of Vpr variants in HIV-1-positive patients. The *vpr* gene was amplified and analyzed, as described in SI-3. (**a**) Nucleotide sequence of clone 10. The nucleotide sequence was compared with that of the prototype NL4-3. Clone 10 has a four-base insertion at nucleotide 81, generating a stop codon within the insert (indicated by the box). Nucleotides that are the same as those in NL4-3 are marked with small bars. (**b**) Amino acid sequences of Vpr variants found in the patients. The amino acids deduced from the obtained sequences and the NL4-3 clone are shown. As described in SI-3a, clone 10 was recognized as a major variant in patient N-10, while clone N was the major variant in patients N-04 and 09.

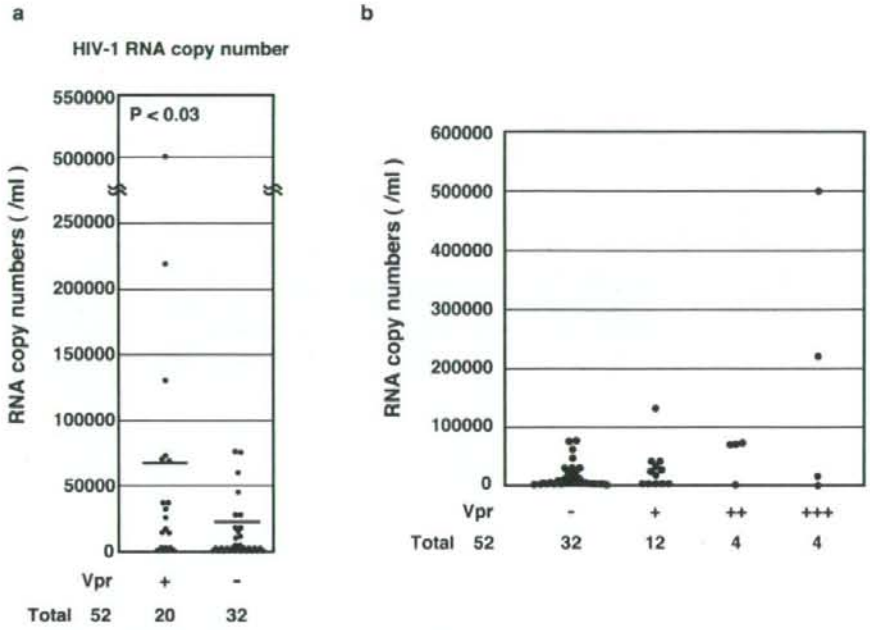

FIG. 3. Correlation between Vpr detection and clinical data. The analyzed cases were divided into Vpr-positive and Vpr-negative groups, and the statistical analysis was done using Student's *t*-test. (**a**). The relationships with the HIV-1 RNA copy number. The bars indicate the mean numbers in each group. The difference for HIV-RNA copy number with Vpr was statistically significant ($p < 0.03$). (**b**) Distribution of Vpr-positive patients according to the concentration of plasma Vpr. Based on the semiquantitative analysis, patients were divided into four groups: Vpr-negative (−), Vpr-positive with less than 1 ng/ml (+), 1–5 ng/ml (++), and more than 5 ng/ml (+++). Each dot means a patient.

TABLE 2. FREQUENCY OF *vpr* VARIANTS IN HIV-1 PATIENTS[a]

	vpr *variants*			
Cases	*NL4-3*	*Clone N*	*Clone 10*	*Mutant-1*
N-03	5[b]	—	9	2
N-04	—	14	—	—
N-05	—	2	3	2
N-09	—	7	—	—
N-10	—	—	6	—
N-12	—	4	—	4

[a]PCR products amplified from patient genomic DNA were subcloned into the vector, and several clones were sequenced. The numbers in the table indicate the frequency of clones encountered in the sequence analyses. All 6 clones derived from patient N-10 were clone 10. In patients N-04 and 09, clone N was identified as the major variant; all 14 clones for patient N-04 and all 7 clones for patient N-09 were clone N. Patients N-03 and N-05 each had 3 *vpr* variants, including the Mutant-1 variant (see Fig. 2b).

[b]Number of analyzed clones.

ACKNOWLEDGMENTS

We thank the healthy volunteers and C. Nakai-Murakami for donating peripheral blood and providing technical assistance. We are grateful for samples of HIV-1-positive patients to Drs. C. Kobayashi (National Hospital Organization Chiba Medical Center), I. Sato (National Hospital Organization Sendai Medical Center), H. Hanafusa (Ogikubo Hospital), J. Matsuda (Teikyo University School of Medicine), M. Sakai (University of Occupational and Environmental Health), S. Ikeda (Sasebo Municipal Hospital), and T. Fujii (Hiroshima University School of Medicine). This work was supported by a Grant-in-Aid for Research on Health Sciences focusing on Drug Innovation from the Japan Health Sciences Foundation Research and Research on HIV/AIDS from the Ministry of Health, Labor and Welfare of Japan. Dr. Sun is a research resident supported by the Foundation for AIDS prevention.

REFERENCES

1. Palella FJ, Delaney KM, Moorman AC, Loveless MO, Fuhrer J, Satten GA, *et al.*: Declining morbidity and mortality among pa-

tients with advanced human immunodeficiency virus infection. N Engl J Med 1998;338:853–860.
2. Finzi D, Hermankova M, Pierson T, Carruth LM, Buck C, Chaisson RE, *et al.*: Identification of a reservoir for HIV-1 in patients on highly active antiretroviral therapy. Science 1997;278:1259–1300.
3. Heizinger NK, Bukrinsky MI, Haggerty SA, Ragland AM, Kewalramani V, Lee M-A, *et al.*: The Vpr protein of human immunodeficiency virus type 1 influences nuclear localization of viral nucleic acids in nondividing host cells. Proc Natl Acad Sci USA 1994;91:7311–7315.
4. Koyanagi Y, O'Brien WA, Zhao JQ, Golde DW, Gasson JC, and Chen ISY: Cytokines alter production of HIV-1 from primary mononuclear phagocytes. Science 1988;241:1673–1675.
5. Heinzinger NK, Bukrinsky MI, Haggerty SA, Ragland AM, Kewalramani V, Lee MA, *et al.*: The Vpr protein of human immunodeficiency virus type 1 influences nuclear localization of viral nucleic acids in nondividing host cells. Proc Natl Acad Sci USA 1994;91:7311–7315.
6. Vodicka MA, Koepp DM, Silver PA, and Emerman M: HIV-1 vpr interact with the nuclear transport pathway to promote macrophage infection. Genes Dev 1998;12:175–185.
7. Jenkins Y, McEntee M, Weis K, and Greene WC: Characterization of HIV-1 vpr nuclear import: Analysis of signal and pathways. J Cell Biol 1998;143:875–885.
8. Levy DN, Refaeli Y, MacGregor RB, and Weiner DB: Serum vpr regulates productive infection and latency of human immunodeficiency virus type 1. Proc Natl Acad Sci USA 1994;91:10873–10877.
9. Levy DN, Refaeli Y, and Weiner DB: Extracellular vpr protein increases cellular permissiveness to human immunodeficiency virus replication and reactivates virus from latency. J Virol 1995;69:1243–1252.
10. Marzio PD, Choe S, Ebright M, Knoblauch R, and Landau NR: Mutational analysis of cell cycle arrest, nuclear localization, and virion packaging of human immunodeficiency virus type 1 vpr. J Virol 1995;69:7909–7916.
11. Muthumani K, Hwang DS, Desai BM, Zhang D, Dayes N, Green DR, *et al.*: HIV-1 vpr induces apoptosis through caspase 9 in T cells and peripheral mononuclear cells. J Biol Chem 2002;277:37820–37831.
12. Muthumani K, Hwang DS, Choo AY, Mayilvahanan S, Dayes NS, Thieu KP, *et al.*: HIV-1 vpr inhibits the maturation and activation of macrophage and dendritic cells *in vitro*. Int Immunol 2004;17:103–116.
13. Muthumani K, Choo AY, Zong Wei-Xing, Madesh M, Hwang DS, Premkumar A, *et al.*: The HIV-1 vpr and glucocorticoid receptor complex is a gain-of-function interaction that prevents the nuclear localization of PARP-1. Nat Cell Biol 2006;8:170–179.
14. Lum JJ, Cohen OJ, Nie Z, Weaver JG, Gomez TS, Yao Xiao-Jian, *et al.*: *Vpr* R77Q is associated with long-term nonprogressive HIV infection and impaired induction of apoptosis. J Clin Invest 2003;111:1547–1554.
15. Rodes B, Toro C, Paxinos E, Poveda E, Martinez-Padial M, Benito JM, *et al.*: Difference in disease progression in a cohort of long-term non-progressors after more than 16 years of HIV-1 infection. AIDS 2004;18:1109–1116.
16. Mologni D, Citterio P, Menzaghi B, Zanone P, Riva C, Broggini V, *et al.*: AIDS 2006;20:567–574.
17. Cavert W, Webb C-H, Balfour HH Jr, *et al.*: J Infect Dis 2004;20:2181–2184.
18. Chui C, Cheung PK, Brumme CJ, Mo T, Brumme ZL, Montaner JSG, *et al.*: HIV-1 VprR77Q mutation does not influence clinical response of individuals initiating highly active antiretroviral therapy. AIDS Res Hum Retroviruses 2006;22:615–618.

Address reprint requests to:
Yukihito Ishizaka
Research Institute
International Medical Center of Japan
1-21-1 Toyama
Shinjuku-ku
Tokyo 162-8655, Japan

E-mail: zakay@ri.imcj.go.jp

AIDS RESEARCH AND HUMAN RETROVIRUSES
Volume 24, Number 3, 2008

DOI: 10.1089/aid.2007.0092

Enhancement of OX40-Induced Apoptosis by TNF Coactivation in OX40-Expressing T Cell Lines *in Vitro* Leading to Decreased Targets for HIV Type 1 Production

YOSHIAKI TAKAHASHI,[1,*] REIKO TANAKA,[1] NAOKI YAMAMOTO,[2] and YUETSU TANAKA[1]

ABSTRACT

OX40, a member of the tumor necrosis factor receptor (TNF-R) superfamily, has been shown to play an important role in the survival of antigen-specific CD4$^+$ T cells. We have previously reported that stimulation of the OX40-expressing and HIV-1 chronically infected T cell line, ACH-2/OX40, with either OX40 ligand (OX40L)-expressing cells or with TNF resulted in the activation of HIV-1 followed by apoptotic cell death. In the present study we found that costimulation via OX40 and TNF-R in OX40-expressing HIV-1-infected T cell lines leads to a marked reduction of HIV-1 production associated with rapid cell death. Since HIV-1-negative OX40$^+$ T cell lines underwent rapid apoptotic cell death after OX40L and TNF stimulation, it was reasoned that the ACH-2/OX40 cell death was unlikely to be due to HIV-1 infection. Furthermore, we found that the OX40-mediated apoptosis of the CD4$^+$ T cell line, Molt-4/CCR5-OX40 (M/R5-OX40), required (1) signals mediated via the cytoplasmic tail of OX40, (2) activation of the caspase cascade, including caspase-8 and caspase-3, and (3) induction of endogenous TNF-α, but not of TNF-β, FasL, or TNF-related apoptosis-inducing ligand (TRAIL), suggesting that this apoptosis occurred indirectly via the TNF/TNF-R system. Finally, a fraction of primary activated CD4$^+$ T cells, expressing high levels of OX40, underwent apoptosis, as revealed by annexin V staining, after cocultivation with OX40L$^+$ cells. These results suggest a new biological role of the OX40L/OX40 system in controlling the fate of activated CD4$^+$ T cells and of controlling HIV-1 infection in inflammatory environments.

INTRODUCTION

OX40 (CD134) is a 50-kDa transmembrane protein that serves as a marker of activated T cells. It is a member of the tumor necrosis factor receptor (TNF-R) superfamily, a family that also includes TNF-R1, TNF-R2, CD30, CD40, CD27, CD95 (Fas), TNF-related apoptosis-inducing ligand receptor (TRAIL-R) 1, and TRAIL-R2.[1–3] Its ligand, in humans, OX40L (CD252), was originally identified on human T cell leukemia virus type-1 (HTLV-I)-infected T cell lines and was termed gp34.[4,5] OX40L belongs to the tumor necrosis factor (TNF) superfamily[6] and is expressed predominantly on normal activated dendritic cells (DCs),[7] B cells,[8,9] vein endothelial cells,[10] and stimulated monocytes.[11] OX40-mediated costimulation of CD4$^+$ T cells by OX40L induces nuclear factor-kappa B (NF-κB) activation through TNF-R-associated factor (TRAF)2 and TRAF5,[12] and is associated with a number of immune function activities. These include the enhanced synthesis of T helper (Th) 2 responses from naive CD4$^+$ T cells,[13–15] the production of both Th1 and Th2 cytokines,[16–18] the development and survival of memory CD4$^+$ T cells,[17] the prevention of peripheral CD4$^+$ T cell tolerance,[19] and the ability to block the inhibitory activity of CD4$^+$ CD25$^+$ T regulatory cells.[20] Ligation of OX40L on activated B cells and on immature DC, *in vitro*, results in enhanced immunoglobulin production[9] and maturation of DC,[7] respectively. In addition to these costimulatory functions, additional OX40/OX40L functions include not only the promotion of cell-to-cell adhesion between activated or HTLV-I$^+$ leukemic CD4$^+$ T cells and OX40L$^+$ vein endothelial cells,[21] but also the migration of CD4$^+$ T cells to B cell follicles in pe-

[1]Department of Immunology, Graduate School of Medicine, University of the Ryukyus, Okinawa 903-0215, Japan.
[2]AIDS Research Center, National Institute of Infectious Diseases, Tokyo 162-8640, Japan.
*Present address: AIDS Research Center, National Institute of Infectious Diseases, Tokyo 162-8640, Japan.

ripheral lymph nodes.[22] The failure to properly control OX40/OX40L interaction has been suggested to cause immune abnormalities such as autoimmune diseases,[23–25] allergy,[26,27] or defective protection against pathogens.[15,28–30]

In addition to its ability to induce cell activation, the TNF-R superfamily is also associated with promoting cell death. One group of the TNF-R superfamily, consisting of Fas, TNF-R1, TRAIL-R1, and TRAIL-R2, mediates cell death through their intracytoplasmic death domain (DD). A second group, consisting of the DD-lacking receptors, TNF-R2, CD27, CD30, CD40, 4-1BB, and OX40, is capable of inducing cell death under certain conditions. Thus, for example, activation of TNF-R2 triggers apoptosis of a rhabdomyosarcoma cell line and of HeLa cells.[31] The activation of CD27 induces apoptosis of B cell lines[32] and the activation of CD30 by specific antibody mediates apoptosis of an anaplastic large cell lymphoma[33] and of a T cell hybridoma costimulated with anti-T cell receptor (TCR).[34] In addition, the activation of CD40 by antibody induces apoptosis in transformed cell lines and in normal activated $CD4^+$ T cells costimulated with anti-CD3 antibody.[31,35] The precise mechanisms of cell death induced by the DD-lacking TNF-R superfamily remain to be elucidated. Recently, it has been shown that TNF-R2 stimulation causes TNF-R1-dependent apoptosis by the depletion of the antiapoptotic proteins TRAF2 and IAP.[36,37] We have previously shown that OX40 stimulation activates human immunodeficiency virus type-1 (HIV-1) production in the chronically HIV-1-infected T cell line ACH-2/OX40 through the activation of NF-κB.[38] This mechanism is consistent with another member of the TNF-R superfamily, CD30.[39] Following stimulation with either OX40L or TNF, ACH-2/OX40 cells undergo not only HIV-1 activation but also apoptotic cell death within 48 h.[38]

In the present study, we examined the fate of cells following either OX40 stimulation alone or stimulation with OX40 in combination with TNF. Surprisingly, costimulation resulted in a marked decrease of HIV-1 production, as a consequence of rapid cell death of the T cell line. The cell death was reasoned not to be secondary to HIV-1 infection since OX40 stimulation alone and/or costimulation with TNF also induced cell death of HIV-1-negative T cell lines. Furthermore, the cell death in the T cell lines via OX40 stimulation was mediated indirectly by the TNF/TNF-R system. These observations suggest a new immunological role of OX40.

MATERIALS AND METHODS

Reagents

The medium used consisted of RPMI 1640 medium (Sigma, St. Louis, MO), supplemented with 10% fetal calf serum (FCS; Sigma), 100 U/ml of penicillin, and 100 μg/ml of streptomycin (hereinafter called RPMI medium). Antihuman (h) CD3 (clone OKT-3) and anti-hCD4 (clone OKT-4) monoclonal antibodies (mAbs) were purchased from the American Type Culture Collection (Rockville, MD). Anti-hOX40 mAb (clone B-17D8; mouse IgG2b, κ) was newly generated by a previously described method.[38] Anti-hTNF-α, anti-hTNF-β, and anti-hTRAIL mAbs, for neutralization, were purchased from R&D (Minneapolis, MN). Anti-hFasL neutralizing mAb was purchased from BD Pharmingen (San Diego, CA). Anti-hCaspase-8 and anti-hCaspase-3 mAbs were purchased from Cell Signaling (Danvers, MA) and horseradish peroxidase (HRPO)-conjugated goat antimouse immunoglobulin G (IgG) Ab was purchased from Chemicon (Temecula, CA). Anti-hOX40L neutralizing mAb (clone 5A8)[40] and isotype control mouse IgG1 (mIgG1), anti-HTLV-I Tax mAb (clone TAXY-8),[41] have been described previously. Isotype control mIgG2a and mIgG2b were purchased from BD Pharmingen and ImmunoTools (Friesoythe, Germany), respectively. Recombinant human TNF-α (rhTNF-α), TNF-α (rhTNF-β), interleukin-4 (rhIL-4), and rhIL-12 were purchased from Peprotec (London, UK). rhIL-2 was purchased from Shionogi Pharmaceutical (Osaka, Japan). The broad-spectrum caspase inhibitor, z-VAD-fmk, was purchased from MBL (Nagoya, Japan), dissolved in dimethyl sulfoxide and diluted in medium prior to use. Apoptosis was assessed by the annexin V-fluorescein isothiocyanate (FITC)/propidium iodide (PI) staining kit (Sigma and R&D). The hTNF-α sandwich enzyme-linked immunosorbent assay (ELISA) kit was purchased from R&D. The advanced protein assay reagent was purchased from Cytoskeleton (Denver, CO).

Cells

The hOX40-transfected and the HIV-1 chronically infected human T cell line cells, ACH-2/OX40 (cell groups 4 and 10), and its vector control, ACH-2/control (mock), and the hOX40L-tranfected mouse SV-T2 cell line, SV-T2/OX40L (gp34), and its vector control, SV-T2/control (mock), have been previously described.[38] The cell lines utilized for transfections of OX40, OX40L, and control vector were the human T cell lines Molt-4/CCR5[42] [Molt-4/CCR5-OX40 (M/R5-OX40), -OX40L, and -control], CEM (CEM/OX40, /OX40L, and /control), Jurkat (Jurkat/OX40, /OX40L, and /control), and HIV-1 productively infected human T cell line Molt-4/IIIB [Molt-4/IIIB-OX40 (M/IIIB-OX40), -OX40L, and -control], the human promonocytic cell lines U937 (U937/OX40, /OX40, and /control), THP-1 (THP-1/OX40, /OX40L, and /control), and HIV-1 chronically infected human promonocytic cell line U1 (U1/OX40, /OX40L, and /control), and the human B cell line BJAB (BJAB/OX40, /OX40L, and /control). Aliquots of each of these cell lines were transfected by electroporation of 10–15 μg of the individual plasmids, pCAGIPuro/OX40, pCAGIPuro/OX40L, and control pCAGIPuro, as previously described.[38] In addition, the Molt-4/CCR5 cell line was also transfected with an expression vector containing the OX40 cytoplasmic tail-deleted mutant, pCAGIPuro/OX40-del(6-725), constructed as previously described,[38] to generate Molt-4/CCR5-OX40del cells. For the selection of transfectants, 1 μg/ml puromycin (Wako, Osaka, Japan) was added to the culture media. Expression of OX40 or OX40L in selectively grown cells was determined by flow cytometric analysis, as previously described.[38]

Detection of cell death and apoptosis

SV-T2/OX40L and SV-T2/control stimulator cells were fixed with 4% paraformaldehyde (PFA) for 15 min and washed three times in phosphate-buffered saline (PBS) prior to use. The OX40-expressing responder cells, at 4×10^5 cells/ml, were cocultured with various ratios of PFA-fixed stimulator cells in RPMI medium in the presence or absence of rhTNF-α (2 ng/ml)

or in the presence or absence of rhTNF-β (10 ng/ml) in 48-well culture plates (0.5 ml/well). The cocultures were incubated overnight, or for the indicated periods, at 37°C in 5% CO_2 humidified atmosphere. For blocking of the OX40–OX40L interaction, anti-hOX40L mAb (5A8) was added at a final concentration of 10–40 μg/ml at 37°C for 1 h prior to coculture. In some cases, anti-hTNF-α, anti-hTNF-β, anti-hTRAIL, and anti-hFasL blocking mAbs were added at a final concentration of 30–100 μg/ml at 37°C for 1 h prior to coculture. For inhibition of the caspase-dependent pathways of apoptosis, z-VAD-fmk was included in the culture medium at concentrations of 100 μM. The viability of the responder cells was determined, in triplicate, using a hemocytometer after staining with 0.1% eosin-Y (Wako, Osaka, Japan). The eosin-Y-stained PFA-fixed stimulator SV-T2/OX40L or SV-T2/control cells could be easily distinguished from dead responder cells by their distinct morphology. Apoptotic and necrotic cells were detected by staining with annexin V-FITC and PI, according to the manufacturer's instructions, utilizing a FACSCalibur (Becton Dickinson, San Jose, CA). The data obtained were analyzed using CellQuest software (Becton Dickinson).

HIV-1 production assay

Production of HIV-1 was determined by the measurement of HIV-1 core p24 levels using a commercial ELISA kit (ZeptoMetrix Corporation, Buffalo, NY). Data were analyzed by the Student's *t*-test. To examine the effect of OX40L and/or TNF stimulation on HIV-1 acutely infected T cell lines, M/R5-OX40 and M/R5-control were infected with the HIV-1 molecular clone NL4-3[43] at a multiplicity of infection (MOI) of 0.01 in 0.1 ml for 3 h at 37°C, as previously described.[44] The infected cells were subsequently washed twice and cultured at 2×10^5 cells/ml for 24 h in 48-well culture plates (0.5 ml/well). The infected cells were cocultured with PFA-fixed SV-T2/OX40L or with PFA-fixed SV-T2/control cells at a cell-to-cell ratio of 2:1 in the presence or in the absence of rhTNF-α (2 ng/ml), for an additional 3 days. Cell-free supernatant fluid was collected and the levels of p24 were quantified.

Western blotting

Western blot analysis was performed as previously described.[38] Briefly, M/R5-OX40 cells (4×10^5 cells/well) were stimulated by PFA-fixed SV-T2/OX40L or by PFA-fixed SV-T2/control cells (2×10^5 cells/well) for 6 h in 12-well plates. Cell lysates were obtained by lysis of $2.5–4 \times 10^7$ cells in 1 ml of a lysis buffer (10 mM Tris–HCl, pH 8.0, 140 mM NaCl, 3 mM $MgCl_2$, 2 mM phenylmethylsulfonyl fluoride, 0.5% Nonidet P-40) on ice for 20 min, followed by centrifugation at $13,000 \times g$ for 10 min at 4°C. The cell lysates (6 μg protein/lane) were treated with an equal volume of 2× sample buffer [125 mM Tris–HCl, pH 6.8, 4% sodium dodecyl sulfate (SDS), 20% glycerol, 0.1% bromophenol blue] without 2-mercaptoethanol, separated by SDS–polyacrylamide gel electrophoresis (PAGE), using a 12.5% gel, and then transferred to Immobilon-P Transfer Membrane (Millipore, Bedford, MA). The membrane was blocked with a blocking buffer [1% bovine serum albumin (BSA) in PBS] at 4°C overnight and incubated with the primary anti-hCaspase-8 and anti-hCaspase-3 mAbs (1:1000) according to the manufacturer's instructions. Mem-

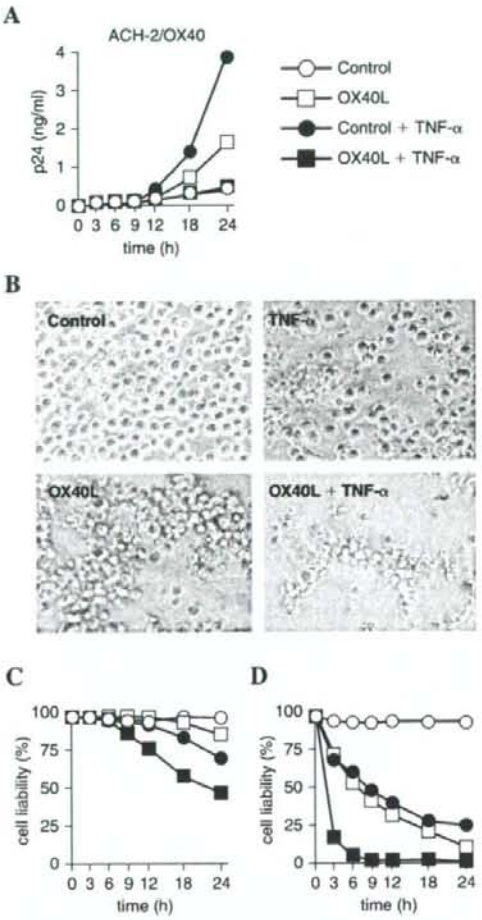

FIG. 1. Marked reduction of HIV-1 production and induction of rapid apoptosis by dual stimulation of ACH-2/OX40 cells with OX40L and TNF. ACH-2/OX40 cells (cell group 10) were cocultured with PFA-fixed SV-T2/OX40L (OX40L) or with PFA-fixed SV-T2/control (Control) cells in the presence or in the absence of TNF-α at 2 ng/ml for 24 h. (**A**) The kinetics of HIV-1 production, as determined by the level of HIV-1 p24 in the culture supernatants, (**B**) microscopic observation of morphological changes, (**C**) the kinetics of cell death as determined by an eosin-Y dye exclusion assay, and (**D**) the kinetics of apoptosis as determined by annexin V/PI staining. Morphological changes were examined under an inverted microscope at 100× original magnification. The cell viability was shown as percentage of control. Representative results from three independent experiments are shown. The data presented are the mean values ± SD of triplicate determinations.

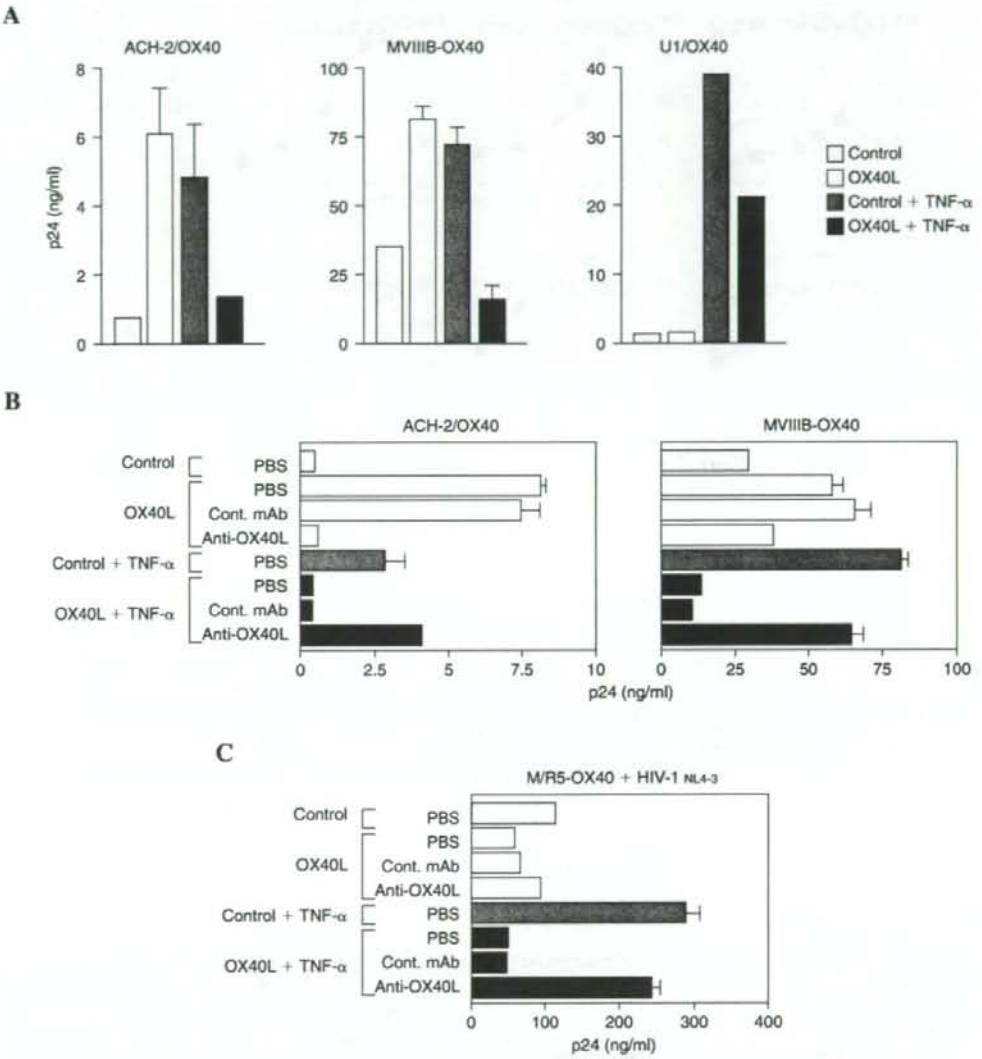

FIG. 2. Reduction of HIV-1 production in various HIV-1-infected cell lines. Several OX40-expressing cell lines were cocultured with PFA-fixed SV-T2/OX40L (OX40L) or with PFA-fixed SV-T2/control (Control) cells in the presence or absence of TNF-α (2 ng/ml) for 24 h. The levels of HIV-1 p24 produced in the culture supernatants were determined by ELISA. (**A**) Representative data was obtained using the HIV-1 chronically infected ACH-2/OX40 cells (cell group 4), the HIV-1 productively infected Molt-4/IIIB-OX40 cells (M/IIIB-OX40), and the HIV-1 chronically infected U1/OX40 cells. (**B**) The blocking effect of the anti-OX40L mAb (Anti-OX40L, 10 μg/ml for ACH-2/OX40 and 40 μg/ml for M/IIIB-OX40), negative control mAb (Cont. mAb, the same conditions as above) or of PBS was determined using ACH-2/OX40 and M/IIIB-OX40 cells. (**C**) The Molt-4/CCR5-OX40 cells (M/R5-OX40) were acutely infected with HIV-1_{NL4-3} at an MOI of 0.01, were precultured for 24 h, and were stimulated with OX40L and/or with TNF for an additional 72 h. The blocking effect of equal volumes of anti-OX40L mAb (Anti-OX40L, 10 μg/ml), negative control mAb (Cont. mAb, 10 μg/ml), or of PBS was determined. The data presented are the mean values ± SD of triplicate determinations. Representative results from three independent experiments are shown.